

Chronic Fatigue Syndrome: A Quantum Mechanical Perspective

Ricardo J. Simeoni

Research and Development, Neurödinger, Sunshine Coast, QLD 4575 Australia.

Corresponding author: Ricardo J. Simeoni (rsimeoni@neurodinger.com, www.neurodinger.com).

1. INTRODUCTION

1.1 GENERAL

Chronic fatigue syndrome (CFS), also known as myalgic encephalomyelitis (ME) or systemic exertional intolerance disease (SEID), is an illness dominated by long-term fatigue persisting for more than six months, incapacitating to the point of sufferers being bedridden or housebound in some cases, and unexplained by some other underlying medical condition. CFS is also often characterised by unrefreshing sleep, post-exertional discomfort ranging from malaise to extreme exhaustion, orthostatic (upright posture) intolerance, muscle pain, cognitive impairment (including the commonly described symptom of "brain fog"), and deterioration in cellular bioenergetics [1–3].

Scientific estimates of the world-wide population percentage that suffer from CFS naturally vary, but a conservative estimate based on several studies is at least 0.4%, thereby equating to millions world-wide [1–4]. Thankfully, after decades of dismissal by some quarters, leading to despair and exasperation of sufferers, CFS is now widely accepted as a legitimate illness. However, while depreciating labels such as "yuppy flu" have subsequently been banished to recent history, this new-found acceptance provides comfort for sufferers only up to a certain point. Viz., CFS is still far from fully understood and is often described as a complex, multisystem illness with no clear pathological mechanisms or diagnostic biomarkers [1–3], from which treatment uncertainty ensues [1,2]. Sadly, due in no small part to this uncertainty and the illness characteristics of the opening paragraph, the suicide rate of CFS sufferers has been reported as approximately seven times that of their healthy counterparts [1,5].

The article *briefly* reviews the medical science of Chronic Fatigue Syndrome and the illness' impact on society, while also sharing a 29-year Case Study with an intriguing hypothesis-based outcome including quantifiable relief. Is this outcome just a one-off mathematical curiosity?, or, will it be verified in the fullness of time as being profoundly grounded in Quantum Mechanics?

The economic and other social impacts of CFS are difficult to determine because of the arbitrariness of case definitions, lack of evidence including prevalence data, diagnostic inability of some physicians due to factors such as disbelief and lack of understanding (one major survey [4] reveals that 62% of sufferers are not confident in their general physician's understanding), and difficulty many sufferers have in explaining the symptoms of their illness (another survey [2] shows that a majority or substantial proportion, depending on factors such as country of origin, have difficulty explaining their illness to not only physicians but also family and friends). Societal impacts of CFS have nonetheless been assessed by various committees

(e.g., associated with the United States' Institute of Medicine) and working/action groups (e.g., associated with the European Union). As expected, the economic impact of CFS is formally declared to be significant, with the net income of a CFS household in Europe being substantially lower than general population households (i.e., individual productivity effect), and the total annual cost burden being tens of billions of dollars in the United States alone [1–4].

1.2 CFS AETIOLOGY

The World Health Organization generally classifies CFS as a neurological illness involving the central nervous system. Some notable and more specific examples of proposed CFS aetiology components are summarised below, with these examples reflecting the complex multisystem nature of CFS and not necessarily being mutually exclusive:

- Recent studies suggest that CFS arises from functional changes in the brain, with spectroscopic and inflammatory brain changes (e.g., following repeated exercise) also demonstrated. However, uncertainty over the character,

An extended version of this superseding article was published May 9, 2022 to support the first World ME Day (themed #LearnFromME) of May 12.

location and propensity of such changes remains and the need for further functional neuroimaging studies is recognised [2,3,6,7].

- A significant increase in red blood cell (RBC) stiffness is reported in CFS, suggesting that compromised RBC transport through microcapillaries may contribute to CFS aetiology and that this diminished deformability could form the basis of a first-pass diagnostic test [8]. Further to this point, the previously identified CFS characteristic of orthostatic intolerance (estimated to occur in up to 97% of cases) is linked to under-oxygenation of the brain to which diminished RBC deformability is thought to be a contributing factor [9].
- Unusual RBC shape, leading to reduced blood flow and changes in molecular docking on the RBC surface, is reported in CFS [10]. The subsequent increase in the number of stomatocytes (RBCs that have lost their typical concave shape, due for example to membrane defect), adds to the previous point of diminished RBC deformability to support poor microcirculation as contributing to CFS aetiology.
- Dysfunction of mitochondria (subcellular organelles within the cytoplasm of aerobic cells) is found in CFS, with the interference of adenosine triphosphate (ATP) production being one of several consequences within the explanatory pathological pathway [11] (ATP is fundamentally essential for cellular-level metabolic energy requirements as outlined in Section 3).
- CFS is largely resolved as *not* being attributable to some ongoing infection, endocrine disorder, or psychiatric condition [3,6]. While some similarly do not assign an immunological disorder attribution, more often over-stimulation or over-reaction of the immune system (hyperimmune response), impaired immune system response, immuno-inflammatory, and oxidative damage to the immune system, are all utilised expressions associated with CFS [3,6,8,11–13], which in several research circles is described as a neuroimmune disease [1,11,14]. This immunological quandary again highlights the complexity of the ongoing medical challenge at hand.

1.3 VIRAL TRIGGERS OF CFS

One clear aspect of CFS is that underlying pathophysiology implicates a range of different acute infections as onset triggers in a *significant minority* of cases (i.e., infections like Epstein-Barr, Ross River and the 2003 outbreak variant of Severe Acute Respiratory Syndrome, or SARS, viruses). No other medical or psychological factors are definitively implicated in CFS [7]. For many observers such triggerings are mindful of, if not directly related to, the crippling fatigue that is widely reported within contemporary media and recent studies as a lasting symptom of COVID-19. Such COVID-

19-triggered CFS has led to the coined phrases of COVID-19 "long-haulers" or "long COVID", and has returned CFS to the public awareness spotlight [12]. However, too familiarly the lack of definitive CFS biomarkers is again confirmed by long COVID research, and sadly the dismissive attitudes of some in the medical profession is also a point of exasperation for long COVID sufferers [12], contributing for example to the in-desperation-establishment of a "long COVID kids" Facebook site in the United Kingdom.

1.4 CFS TREATMENT

Established treatments, such as cognitive behaviour therapy (CBT) and graded exercise therapy (GET), primarily aim to manage the symptoms and improve the overall function of sufferers. The confounding nature of CFS extends to these treatments, since there is wide ongoing debate over their effectiveness [1,15]. For example, while GET is shown to benefit some, for others it is essentially considered just "cruel". A host of alternative treatments, some of which may be described as holistic or naturopathic or similar, naturally also exist, such as cryogenic, floatation and oxygen therapies, to name just a few. It is not the intention or place of the present article to compare, critique or scientifically review such treatments. It will simply be stated that, at least anecdotally, some such treatments seem to bring relief to some individuals (which is a positive outcome for those lucky enough to find any relief), but certainly most do not consider these treatments to be CFS cures or long-term major alleviators for the majority.

Contemporary scientific scrutiny into how COVID-19 can damage the brain [13,16,17], and suggesting that the virus' fatigue and adverse neurological effects (such as loss of smell and taste, altered mental states that can lead to the development of psychoses, and brain shrinkage in regions essential for processing memory, cognition and emotion) are indeed due to some hyperimmune response with neuroinflammation, does however offer many CFS sufferers new hope. Viz., hope that as a result of such scrutiny highly effective treatments (e.g., neural rewiring therapies [16]) and eventual cure await, even with the caveat of caution around some uncertain degree of overlap between COVID and non-COVID CFS.

1.5 ARTICLE PERSPECTIVE AND SCOPE

The present article's title upon first glance likely appears incongruous. However, while some delight was taken in choosing this "humorous-to-a-physicist" title, the article is journalistically serious and does not make light of CFS. Rather, in addition to the above CFS overview, the article reflects upon a presented clinical Case Study of a seemingly recovering CFS sufferer to form a justified CFS hypothesis for future testing.

The to-be-formed hypothesis follows from the unique neuro-perspectives of [18], which explore central nervous system impulse encoding revelations via a new approach to

high-order electroencephalogram (EEG) phase analysis. Given that CFS has a neurological component, can these new perspectives be applied to the area of CFS, and in particular to the to-be-presented Case Study of recovery? While this tangent might seem a long bow to draw, perhaps a fresh CFS perspective is just what is currently needed. Despite the quantum mechanical aspects to come and references [18] and [19], the latter on a discrete oscillator phase noise effect applied within phase-shift keying radiofrequency (RF) digital signal modulation, being recommended prior readings for those with a biomedical engineering or similar background, no such specialist backgrounds are assumed for readers.

In brief, the present article represents academic (science and medicine) journalism that is hopefully considered high-interest, and shares via Case Study the clinical/medical results, collated over several years, for a scientifically dependent individual. The eventually formed hypothesis is intended for testing within a future formalised study, and so presently may be countered by alternative explanatory hypotheses, such as placebo and simple recovery coincidence, which are also identified.

2. CLINICAL CASE STUDY

2.1 GENERAL

The 29 year clinical Case Study (many sufferers of CFS have been living with the illness for over 20 or 30 years [4]) to be shared is that of my own, from CFS onset at 25 years of age to a recovery road at 54 years of age. While journalism (academic or otherwise) in which an Author has a vested interest is not uncommon, and indeed can be beneficial due to the experience and passion that the Author carries (CFS sufferers are considered experts in their own illness and experiences [4]), this declared interest is the reason independence is waived in Subsection 1.5. Despite this declaration, the quantitative and verifiable clinical/medical results to follow will be compelling to some and are presented in the belief that any road-to-recovery story and subsequently formed new hypothesis will always be of interest to CFS sufferers since, like myself, they will have "tried everything" to overcome the illness. However, until the new hypothesis is tested within controlled studies, all interested CFS sufferers are encouraged to retain a degree of healthy scepticism given the existence of other explanatory hypotheses.

A final dependence note is that the Case Study of this Section, and the treatment approach of a later Section, should not be considered "self-experimentation" or formal research (the latter being a standard to which qualification is not sought), but merely a shared chronology of clinical/medical results and details of a particularly desperate effort to return to good health during an individual's CFS journey. However, even if a self-experimentation label was applied, this should not necessarily bring discard given that

respected precedents exist for academic journalism centred around the Author or Commentator as test subject. For example, a popular British Broadcasting Corporation (BBC) production on sleep [20] involves experimentation on the presenter (a physician and multiaward-winning medicine/science journalist) who, in another BBC (series) production [21], explores and in some cases celebrates historical and modern day self-experimenters in medicine. Well-known examples from the series include the intentional consumption of *Helicobacter pylori* (stomach ulcer) bacterium in 1984 with eventual awarding of a Nobel Prize in 2005 (to cut a long story short), and a controversial physician now regarded as being ahead of his time in the 1950s for nutrition research into the importance of essential Omega 3 fatty acids for heart and brain health. The celebrated physician of the latter example in 1979 undertook a 100 day extreme Inuit diet with weekly self-cutting to measure personal bleed times, and within a 1956 letter [22] to the Editor of the *Lancet* writes:

"your readers having stereotyped minds should stop reading at this point", Dr Hugh M Sinclair FCRP.

The present article similarly encourages open-mindedness in regards to quantum findings for a Case Study where the person of clinical focus and presenter are one in the same.

2.2 PRE CFS ONSET

Before the onset of CFS I fell into a common (but not the only) CFS demographic of a fit and motivated young adult from a professional career background, generally making the most of every available minute of the day. In early 1993 I left my professional position and moved to Townsville (in tropical North Queensland) to undertake further postgraduate studies. At the time I had no awareness of viruses such as Ross River Fever and, taking no precautions, allowed myself to be exposed to many mosquito bites (e.g., at social student functions such as evening BBQs). Unsurprisingly, in short time I developed Ross River Fever¹ which was a clear "quantum trigger" for my CFS onset.

2.3 CFS SYMPTOMS

As per the imagery invoked by the previous *quantum trigger* descriptor, the onset of CFS symptoms at 25 years of age was immediate rather than gradual (immediate or gradual onset are both commonly reported in CFS). After an initial acute period of severe symptoms, the long-term symptoms experienced aligned with those previously cited in Subsection 1.1 as classic characteristics of CFS, as well as with several secondary characteristics associated with CFS.

In the earliest years I sought consultation from several physicians but without understanding as per the introductory

¹Barmah Forest virus may also have been contracted around this time since positive antibody test results for this virus were identified some years after Ross River Fever infection confirmation. However, simultaneous status for these mosquito-borne viral infections cannot be stated with certainty.

statistic of Subsection 1.1, and from naturopathic-type clinicians. I recall on one early occasion (within the first 12 months of illness) having to be insistent with a reluctant general physician as to there having to be something wrong due to the severity of fatigue, and the need for a blood test. From 2008 I have also received intermittent consultations (approximately every 18 months) from a CFS specialist physician in South Brisbane. Ultimately these interventions brought no symptom relief, despite the appreciated efforts of the latter-mentioned specialist.

Because I was never permanently housebound and was able to maintain a career and moderate level of fitness (CFS can manifest in varying ways), CFS understanding by some was difficult. Certainly, many other CFS sufferers and sufferers of other medical conditions have faced significantly greater health challenges than myself, and so appreciation of my relative good fortune is not lost. Nonetheless, it would be wrong to dismiss the detrimental impact that CFS has on the lives of millions who suffer from CFS to a similar extent (i.e., not to the extent of being housebound), since a significant degree of debilitation is still experienced, leaving such sufferers feeling continually "weighted down" and as if they have ran a marathon after pushing through each and every day.

The long-term authenticity and severity of my condition is supported by the clinical/medical results shared within the following Subsections.

2.4 SELECT CLINICAL/MEDICAL RESULTS

Subsections 2.4.1 to 2.4.4 give a glimpse of the copious medical testing undertaken over the years to which all CFS sufferers can relate (many other tests have been undertaken but are not included here due mostly to their negative finding, or findings nonessential to the shared CFS story). Urine and gut analyses of the first two of these Subsections naturally will have advanced since their time of reporting in 1998, however the results are still informative.

2.4.1 URINE ANALYSIS, UNIVERSITY OF NEWCASTLE, AUSTRALIA, 1998

The following abridged results are extracted from a urine analysis report prepared by the Department of Biological Sciences, University of Newcastle, Australia, August 1998 (sample ID 4114, Entry 4228) within a CFS research program (with commercial arm) and associated support network that are no longer in existence. The urine analysis especially examines amino and organic acid metabolic disturbances (amino acids being the building blocks of proteins).

A summarising urine excretion profile of particular interest from the above report is given in figure 1 and includes diagnostic outcomes such as a 10 rating (on a 0 to 10 scale) for myofibrillar catabolism, and an above 8 rating for one particular fatigue classification. These indicating results for the first time (five years after CFS onset) brought

hope and a certain degree of self-assurance and vindication that what was being experienced was not some "yuppy flu" or state of mind to be dismissed. Ratings of 10 and >8 were certainly subjectively consistent with my daily feeling of fatigue for 29 years. It is unfortunate that these CFS analysis services, that were arguably ahead of their time, were discontinued rather than further developed, however this discontinuation no doubt reflects the many complex facets of CFS.

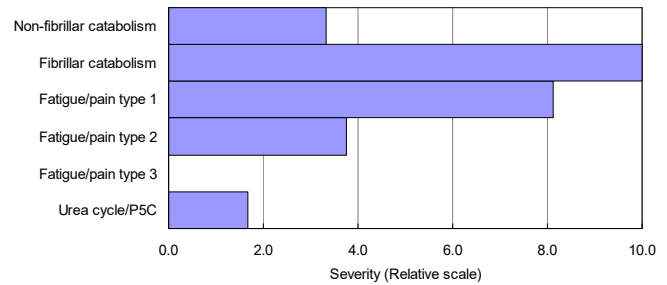


FIGURE 1. Urine excretion profile, with relative 0 to 10 unit scale, consistent with amino acid metabolism disturbances in subjects presenting with persistent pain or fatigue (graphic recreated from original report identified in-text).

The full University of Newcastle report also rates the excretion levels of urine constituents in relative percentage terms, with percentage values simply classified as low, average or high (no doubt to aid readability by the patient). Table 1 gives such values for select (4 out of 28) constituents of interest, with average population values bracketed for comparison (no population percentile ranges or standard deviations are quoted within the original report):

Table 1. Levels in relative percentage terms of select urine constituents, with bracketed values representing expected population averages.

Constituent	Low	High
Citric acid		11.69 (0.74)
Succinic acid	0.34 (1.37)	
3-Methyl-histidine		10.03 (1.33)
Lysine		8.27 (2.34)

According to the original University of Newcastle report, the relatively low and high excretion values for succinic and citric acids respectively, as seen in table 1, are together characteristic of CFS/pain and may be representative of disturbances in the Krebs cycle (high citric acid excretion levels, here approximately 16 times the population average, may remove divalent cations of elements such as magnesium, Mg). Note that from this point chemical symbols only are used to introduce elements within text. Note also that the Krebs cycle, alternatively known as the tricarboxylic acid (TCA) or citric acid cycle, is further briefly addressed within Section 3.

Also within table 1, 3-Methyl-histidine (3MH), or at least its analogue histidine, is an amino acid present in actin and myosin such that approximately 90% of human 3MH is contained within skeletal muscle². Table 1 shows high 3MH excretion which can indicate muscle protein turnover or catabolic breakdown of myofibrillar protein (e.g., in the instance of muscle injury) [23,24]. The high lysine excretion indicated in table 1 associates with the "type 1" fatigue of figure 1.

The above-noted amino acid metabolic disturbances, including myofibrillar protein breakdown, along with evidence of Krebs cycle disturbances, will be revisited as the present article continues to build towards its eventual hypothesis.

2.4.2 GUT ANALYSIS, UNIVERSITY OF NEWCASTLE, AUSTRALIA, 1998

In parallel with the above urine analysis, a gut health analysis was also undertaken through the University of Newcastle, the reporting for which states that alterations in excreted lipid composition and aerobic/anaerobic microflora (microbiota) distribution occur in CFS. Such occurrences are perhaps generally unsurprising, given the known association between good gut health and a robust immune system, as well as the association between CFS and immunological dysfunction.

The majority of the University of Newcastle's gut analysis report will not be presented here (due more to being non-essential to the eventually drawn hypothesis), other than to briefly mention one of the several out of balance findings. This finding being coprostanol lipid (1 of 27 reported lipids) excretion being approximately 150 times lower than the population average with a coprostanol-to-cholesterol ratio of only 0.17%. This ratio value is particularly interesting and potentially telling of a compromised system. For most, the efficiency of converting cholesterol into coprostanol (via microflora metabolism) is generally high, such that minority "low converters" (ratios of < 0.5%) account for 5 to 30% of the adult population [25]. That recent study further highlights that low conversion efficiency may signify a higher risk of disease and loss of good health (though the adverse association is still not extensively assessed).

2.4.3 OLIGO SCAN (2021)

The Oligo scan (marketed as Oligoscan within industry) reports on mineral, vitamin and heavy metal levels in body tissue including peripheral blood vessels, and is based on rapid four-point spectroscopic analysis of the hand. The scan is relatively new to Australia where it is becoming increasingly popular within naturopathic and holistic

practices, some of which also offer conventional medical services. The scan is intended as an indicating tool for trained clinicians who naturally would complement any indications with other relevant whole-picture clinical evidence. The diagnostic wherewithal of the scan's overall report is arguably not fully accepted (or necessarily claimed) from an academic research perspective, and the present article commences with a neutral position as to any such capability.

Within the Oligo scan's mineral test report (the first main component of the overall report), the levels of 21 elements are generated, as per figure 2a which displays my results from a January 19, 2021 scan performed by a Brisbane-based clinic (commercial provider). Of the 21 elements analysed, P was revealed as the only element at a low minus or "red" level. Figure 2b shows a consistent P finding within a scan independently repeated approximately seven months later on August 16, 2021 by a separate Brisbane-based clinic.

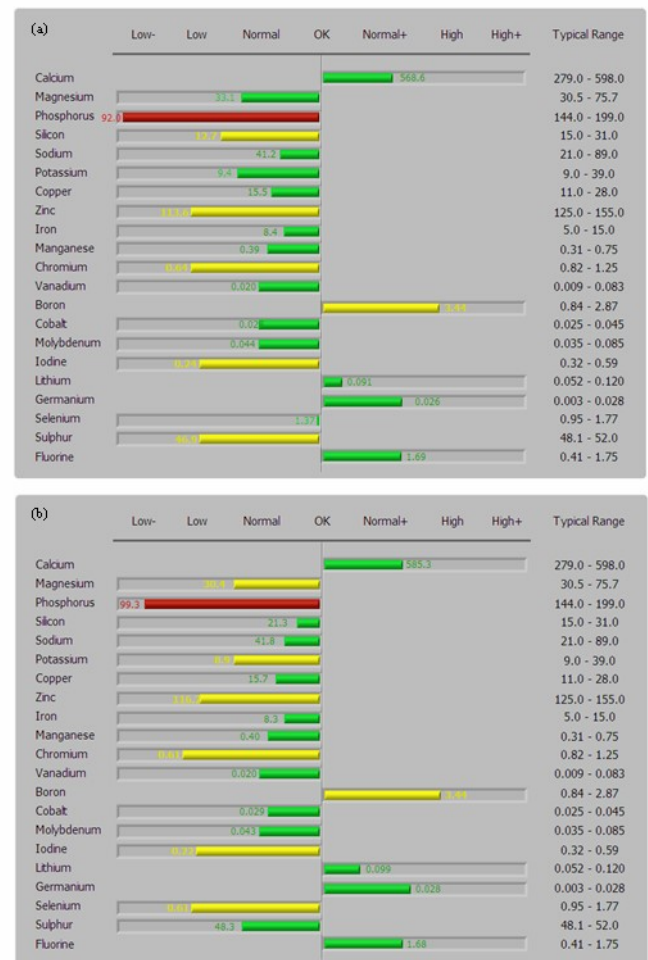


FIGURE 2. Oligo scan report (first main component of) which displays body tissue levels of 21 specified elements, as independently obtained on (a) January 19, 2021 and (b) August 16, 2021. Graphics have been regenerated from the original clinical reports which do not specify the units of elemental levels.

²Myofilaments are organised into bundles called myofibrils and largely consist of the *contractile* proteins actin (thin filaments) and myosin (thick filaments). However, other important constituent proteins exist such as for thin filaments the *regulating* proteins tropomyosin and attached troponin (complex). Tropomyosin interacts with actin, myosin and troponin to regulate muscle contraction and relaxation (i.e., controls filament sliding), a process for which Ca⁺⁺ binding to troponin in response to action potential-induced Ca⁺⁺ concentration changes is key.

The scan results of figure 2 were obtained under a subjectively considered balanced diet that routinely included foods relatively high in P. Note that while over the years I have tried taking health supplements, under health or medical practitioner guidance, I have never experienced a perceived beneficial CFS alleviatory effect from such supplements (which I can have intolerance towards, including instances of fatigue exacerbation which does not pass with persistence). Hence, no supplements were taken in the months leading up to these Oligo scans. Indeed, over the years I have formed the *unqualified* opinion that CFS is very complex (universally accepted as being the case) and so for many, or certainly in my case, a prescribed supplemental remedial approach unfortunately does not provide the "simple answer" (else for example, such remedies would have already been identified by the medical support teams of high-profile CFS sufferers in fields such as professional sport, and by the many CFS studies across the world-wide tertiary landscape). Naturally, taking health supplements under the broad umbrella of fatigue is beneficial and even essential to many, including some other CFS sufferers, and in no way does the present article discourage their use (as always, individual effects vary and decisions on the use of such supplements must always be made under the guidance of a qualified health practitioner).

As indicated above, there is some reservation about the scientific efficacy of the Oligo scan for academic research (e.g., as raised within academic on-line discussion forums), and indeed taking a wait-and-see approach until supporting (or otherwise) scientific evidence grows is probably prudent for such formalised research. However, one cannot help but be impressed by the consistency between figures 2a and 2b, the scans for which were independently undertaken seven months apart at different clinics unaware of the other clinic's scan (i.e., consistencies such as elements P and B markedly displaying the lowest and highest levels respectively, as well as several easily identified others).

The consistent low minus P result in figures 2a and 2b, for a well balanced diet relatively high in P, is naturally of interest for a sufferer of CFS, given that P plays a critical role within body energetics (see Section 3). In this regard it is noteworthy that over the years spanning my CFS, conventional blood tests have always shown blood P levels to be within a normal range (perhaps representative of blood levels not always being indicative of cellular tissue levels for some elements [26]). As per the University of Newcastle findings of Subsection 2.4.1, this Oligo scan-based P finding will be revisited as the present article continues to build towards its eventual hypothesis.

2.4.4 MISCELLANEOUS CONVENTIONAL BLOOD PATHOLOGY

The following blood pathology³, with results outside of typical (bracketed) ranges, have been reported by Queensland Medical Laboratories at the request of the aforementioned CFS specialist physician:

Ferritin (Fe-storing protein)

- Nov 2015, Dec 2015, Jan 2020
- 354, 327, 349 (30 – 320) $\mu\text{g}\cdot\text{L}^{-1}$ respectively
- Mild elevation with no supplement intake
- Dec 2015 PCR test for hereditary haemochromatosis gene negative (C282Y, H63D, S65C mutations not detected)

Serum Vitamin D (1,25-dihydroxy vitamin D)

- July 2008
- 156 (40 – 150) $\text{pmol}\cdot\text{L}^{-1}$
- Mild elevation with no supplement intake and quite limited sun exposure.

3. POSSIBLE SIGNIFICANCE OF VERY LOW PHOSPHOROUS – "ENERGETICS 101"

Amidst all of the scientific debate, uncertainty, and points of view in regards to CFS, ultimately what is undeniable is the simple perspective that a person suffering CFS is somehow deficient in energy or the ability to effectively utilise available energy. When postulating a new CFS hypothesis, it is therefore reasonable to consider the origins of biological energy production. That is, all students of science are familiar with the notion of energy production from respiration, which involves the release of chemical energies from foods such as glucose. However, at its core this fundamental and well understood process involves P, especially in the form of ATP. For example, within both the aerobic and anaerobic equations of respiration, high-energy ATP is synthesised from adenosine diphosphate (ADP), with the synthesised ATP providing for cellular-level metabolic energy requirements (since stored chemical energy is then available via ATP splitting into ADP plus a cleaved inorganic P) [27].

In the case of skeletal muscle, ATP-sourced mechanical energy provides for the cross-bridge interactions, between actin and myosin filaments, that result in the production of muscular contractile force. The resynthesis of ATP from ADP and inorganic phosphate continually occurs within muscle cells via three main energy systems, namely the *Immediate, Anaerobic (Lactic Acid)* and *Aerobic (Oxidative)* systems. The latter Aerobic system provides a relatively slow rate of ATP production for endurance activities. Fats (fatty acids), proteins (amino acids) and carbohydrates (glycogen and glucose) can all be aerobically metabolised to

³Laboratory reference numbers in the order of listing are: 15-71216303-ISM-0, 15-72141582-ISM-0, 20-71814636-ISM-0, 15-69998378-HFE-0, and 08-7028292-VDD-0.

produce ATP (with the metabolic pathways involving the Krebs cycle)⁴. Aerobic ATP production occurs in the mitochondria, and so not surprisingly mitochondrial dysfunction (e.g., lowered ATP production, *impaired oxidative phosphorylation* and mitochondrial damage) is found in CFS [11].

As well as being a major component of ATP and thus arguably being the most important element in terms of biological energy production as summarised above, P is also an important component of cell membranes and ribonucleic acid (RNA) which is synthesised by DNA in cells. So when a Case Study of a CFS sufferer of almost 30 years repeatedly returns a consistent 21 element body mineral analysis test result, whereby the only element in the low minus or red region is P (as presented within Subsection 2.4.3), and impaired oxidative phosphorylation is associated with CFS [11], the result should reasonably be considered CFS-indicative, especially when supported by other long-term diagnostic findings which include the maximum "10" and ">8" urine analysis ratings from the University of Newcastle analysis. Accordingly, the present article is building towards a CFS mechanistic (plus treatment) hypothesis involving inadequate metabolism of P (and symbiotically associated elements), but also with a quantum mechanical basis as indicated by the article's title. Before arriving at this final hypothesis, further hypothesis framework components are required (Sections 4 and 5).

4. NEW HIGH-ORDER PHASE ANALYSIS OF THE EEG AND ITS QUANTISED FINDINGS

Before reading this Section, those without a biomedical engineering or similarly mathematically-underpinned background are directed to introductory signal processing texts that address the topic of frequency domain, particularly in relation to the electroencephalogram (EEG) or "brain wave" analysis.

4.1 OVERVIEW OF NEW ANALYSIS TECHNIQUE

A promising EEG analysis technique [18] commences with the double application of high resolution Fourier analysis, whereby the second Fourier transformation is applied to an amplitude versus frequency spectrum of a conventional transformation. This technique generates new harmonics spanning the conventional frequency spectrum, in turn allowing profiles of new harmonic phase, ϕ , to be constructed over an effective time-domain, t' (i.e., the double application reverts to some quasi time-domain). The ϕ versus t' behaviour of such profiles generally displays strong linearity for EEGs collected during deep sleep. However, for awake and other stages of sleep, such profiles display many structured ϕ changes. These discrete ϕ changes, or $\Delta\phi$, are found to cluster, with influential $\Delta\phi$ clustering categorised by [18] into ten "Families". Eight of the Families are considered

primary and display $\Delta\phi$ clustering about $\Delta\phi_c = 5^\circ, 10^\circ, 20^\circ, 30^\circ, 50^\circ, 90^\circ, 180^\circ, 270^\circ$. The remaining two Families are considered secondary and display $\Delta\phi$ clustering about $\Delta\phi_c = 135^\circ$ and 220° . The typical chaotic-like nature of conventional first-order EEG harmonic phase analysis is in stark contrast to the highly structured phase behaviour of the described new harmonics.

4.2 MORE SPECIFIC PHASE STRUCTURE FINDINGS OF NEW TECHNIQUE

In many instances within Family $\Delta\phi$ clusterings, the separations between $\Delta\phi$ values are also highly structured and may be written in terms of integer, or fractional-integer, multiples of a proposed quantum increment value, α , with $\frac{1}{2}$ and $\frac{1}{4}$ but especially $\frac{1}{2}$ being fractional examples. A *transition diagram* that graphically displays these $\Delta\phi$ separation multiplicities is given in [18] for each Family, along with the mean α value, $\bar{\alpha}_{\Delta\phi}$, for each Family.

Interestingly, several paired combinations of Family $\bar{\alpha}_{\Delta\phi}$ values form ratios that align with simple common fractions (e.g., $\frac{2}{3}, \frac{1}{5}, \frac{4}{5}$) to high degrees of precision and, as also briefly raised within [18], intriguing linkage can also be made between such formed ratios and ratios of the culturally/historically significant pentatonic music scale and ratios utilised within the communication systems of intelligent mammals such as sperm whales.

Family $\bar{\alpha}_{\Delta\phi}$ versus $\Delta\phi_c$ values display strong parabolic functionality ($r = 0.99998, p < 0.001, 95\% \text{ CI}$) given by:

$$\bar{\alpha}_{\Delta\phi} = (1.9772 \pm 0.0049) \times 10^{-4} \Delta\phi_c^2 - (9.990 \pm 0.097) \times 10^{-3} \Delta\phi_c + (3.002 \pm 0.021) \times 10^{-1}, \tag{1}$$

and as graphically shown by figure 3.

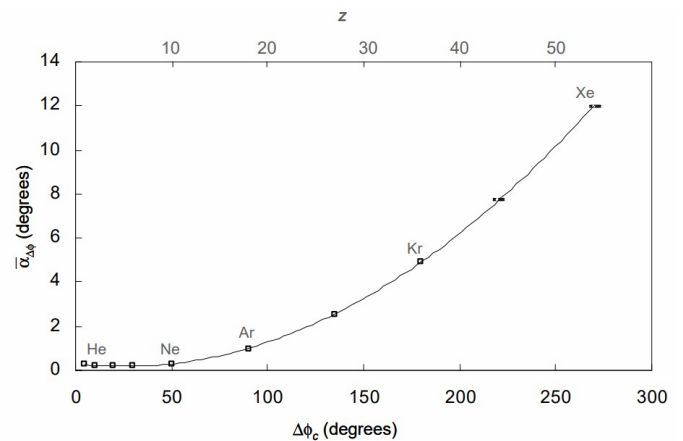


FIGURE 3. Family $\bar{\alpha}_{\Delta\phi}$ versus $\Delta\phi_c$ as presented in [18]. The secondary x-axis applies the linear transformation $\Delta\phi_c/5 \rightarrow z$, with subsequent annotations identifying z values for (five of eight) primary Family members that coincide with the atomic numbers of indicated noble (rare) gases. Error bars (95% CI) are resolvable (just) for the two right-most points only.

⁴Carbohydrates can additionally be anaerobically metabolised within the Krebs cycle.

Within the figure 3 parabolic function, the high precision y -value of the turning point (minimum) corresponds to $\bar{\alpha}_{\min} = 0.174019 \pm 0.000010^\circ$, and is representative of a seemingly universal quantum increment value that spans across Families. Viz., several occurrences of separations between $\Delta\phi$ values being structured in terms of α_{\min} multiples are identified within the $\Delta\phi$ clusterings (transition diagrams) of all Families [18]. The secondary x -axis and annotations of figure 3 are explained within Subsection 4.3.

4.3 QUANTUM MECHANICAL ASPECTS OF PHASE STRUCTURE FINDINGS

The above-described structuring of the separations between $\Delta\phi$ values in terms of $\bar{\alpha}_{\Delta\phi}$ multiples is quantum-like, in that any preference for *half-* or *full-integer* multiplicity is consistent with various forms of quantisation observed in many well-known quantum systems. This identified characteristic, together with other identified quantum-like characteristics including parabolic functionality which is present in various forms within several of the well-known quantum systems, led to the suggestion in [18] of a quantum mechanical governance to neural impulse generation. Hence, within [18] it was concluded that the EEG is encoded by quantised phase transitions between the newly-identified harmonics, allowing for powerful phase-shift keying impulse encoding complexity with high transitional degrees-of-freedom.

A preliminary but nonetheless intriguing offshoot quantisation finding in [18] involves the transformation of primary Family $\Delta\phi_c$ values. Viz., linear mapping to a proposed dimensionless index, z , via the transformation $\Delta\phi_c/5 \rightarrow z$ (as per the secondary x -axis of figure 3), respectively yields for the eight ascending primary Family members $z = 1, 2^*, 4, 6, 10^*, 18^*, 36^*$ and 54^* , where the asterisked z values equate to the atomic numbers, Z , of the noble (rare) gas elements of He ($1s^2$), Ne ($2p^6$), Ar ($3p^6$), Kr ($4p^6$), and Xe ($5p^6$) which are annotated within figure 3 (bracketed notation here gives the filling of the outer-most subshell for indicated elements). Following the same atomic labelling, the remaining primary Family $z = 1, 4, 6$ values equate to the elements of H ($1s^1$), Be ($2s^2$), and C ($2p^2$). It was subsequently also concluded in [18] that this mapping is possibly suggestive of neuro-quantum processes involving elementally-proportional optimal quantum states.

Another linear mapping outcome of intrigue applies to the turning point of the figure 3 parabola (recall that its high precision y -value is representative of a seemingly universal quantum increment value, α_{\min} , that spans across Families). The corresponding x -turning point value, $\Delta\phi_{\min} \approx 25^\circ$, upon transformation yields $z \approx 5$ (or 5.07 ± 0.05 and see [18] for the reason α_{\min} is known to higher precision than $\Delta\phi_{\min}$), and so elemental labelling of $\approx B$ ($2p^1$). Contextual interest in B corresponding to the governing parabola's most important point, arises from the consistently high B finding

in Subsection 2.4.3, and B's significance not only within biological health, but also within geology and astrobiology on the basis of being a likely necessary component for the formation of Earth-like planetary life due to a RNA synthesis role [28].

5. THE MODERN ETHER

The present article is gradually building to a later justified hypothesis considering the possibility that for a minority of people and in certain (e.g., compromised) circumstances, constant exposure to a "modern-day ether" may compete with the complex phase oscillations and encodings of the neural processes of Section 4, and that this competition may not always be completely tolerated. Relevant background to the modern-day ether is thus given below.

5.1 PHILOSOPHICAL UNDERPINNING FOR POSSIBLE BIOLOGICAL INTERACTION

It is indisputable that radiofrequency (RF) electromagnetic waves can influence the human body, since MRI is based on the resonant absorption of RF energy by billions of protons in the body, especially protons belonging to the hydrogen atoms of water molecules. This resonant energy absorption is facilitated by proton precession being undertaken at the same frequency as that of the applied RF waves, with the precession brought about by an applied strong magnetic field that is synonymous with MRI. The resonant RF energy absorption excites the protons to a higher energy state and synchronises the protons' phases of precession (which is "MRI 101"). That is not to say that such RF energy absorption examples are biologically harmful to humans, on the contrary MRI is known for its safety. At the other end of the spectrum, United States officials believe that the deliberate recent targeting of some diplomats via a high-powered electromagnetic weapon, likely operating towards the microwave end of the RF range, has affected their neurological health to the point of brain injury. Clearly then, RF waves can influence the human body, usually in benign ways but also up to seriously adverse ways.

For the less extreme case of MRI RF waves, and more generally RF communications across the board within radio (AM/FM/digital)⁵, cell phone and television broadcasting, the wavelengths of RF waves are physically of the orders of meters to centimeters (even extending to millimeters for new 5G technology). For example, an FM radio broadcast at 100 MHz corresponds to a RF wavelength of around 3 m. Hence, invisible oscillating waves of electromagnetic energy, on a macroscopic scale of physical relevance (i.e., with dimensions relatable to the every-day human macroscopic world), form part of the "modern RF ether" (from this point referred to as the modern ether) that is all around us and which permeates our beings. Again, this modern ether, which has been ever-"thickening" since

⁵The acronyms AM and FM respectively represent amplitude and frequency modulation.

Marconi's development of the wireless telegraph and invention of the radio in the 1890s, should be considered relatively biologically safe, and the research-grounded reports of professional bodies (such as the World Health Organization, Australian Radiation Protection and Nuclear Safety Agency, and International Commission for Non-ionising Radiation Protection) should rightly form the basis for society's position on RF exposure and safety. Of course an individual choosing to minimise and/or avoid unnecessary exposure to RF emissions is also completely reasonable.

The present article takes with seriousness its essential position that any writing under the banner of possible RF electromagnetic interactions with the human body needs to be measured and not alarmist or sensationalised; the article will not be suggesting that every-day RF exposure is routinely biologically damaging and, as per the above commentary, advocates a default to the stated governing authorities for society's guidance on safety surrounding telecommunication issues. Nonetheless, humans are electromagnetic beings in the sense that we generate low level electromagnetic emissions from the electrical activity of the brain and related neurophysiological processes, and the above essential position does not exclude reasoned discussion on the possibility of some form of interaction between the human body and the modern ether, even if interaction is just on some inert level like in MRI (with recognition that biological interactions within the MRI analogy are facilitated by strong magnetic fields which are not present in every-day life). Similarly, the possibility that for a minority and in certain compromised circumstances, constant exposure to the modern ether may compete with the complex neural phase oscillations and encodings of Section 4, and that the competition may not always be completely tolerated, should not be discounted. An aspect of RF telecommunications considered particularly relevant for later hypothesis justification follows.

5.2 INTRODUCTORY THEORY OF STANDARD FREQUENCY MODULATION IN TELECOMMUNICATION

Within standard FM theory, modulating a carrier RF signal's frequency by an amount proportional to the amplitude of the primary signal (such as an analog voice recording) to be broadcasted, also effectively modulates the phase of the carrier RF signal. In addition, the modulation of phase can produce a noise effect in the frequency-domain [19] and phase oscillations can be expected within the (secondary) harmonics of this domain. Thus, even with deliberate phase-shift keying schemes used within modern digital RF communications placed aside, standard RF communications are rife with phase modulations. An overview of standard FM theory that aids in the understanding and quantification of its main inherent phase modulations is given below.

An FM signal of instantaneous amplitude, e , and which is modulated sinusoidally (artificial construct for demonstration purposes), can be written as:

$$e = E \sin(2\pi[f_c + \Delta F \sin(2\pi ft)]t), \tag{2a}$$

where E is the maximum amplitude of the carrier wave, f_c is the unmodulated carrier wave's frequency (e.g., 100 MHz), ΔF is the peak deviation or swing of the carrier frequency away from f_c , f is the modulation frequency for the example case of simple sinusoidal modulation, and t is time (in practice, f_c is modulated in a more complex manner representative of the irregular modulations within speech, music, or other waveform for broadcast).

Routine trigonometric manoeuvring allows (2a) to be re-expressed as:

$$e = E \sin(2\pi f_c t + \varphi), \tag{2b}$$

wherein $\varphi = 2\pi\Delta Ft \sin(2\pi ft)$ represents a modulation in phase (i.e., f_c modulation effectively produces a phase modulation for a constant f_c).

Although the modulations of real-life FM transmissions are more complex than in (2b), real-life modulations nonetheless occur between the discrete limits of $\pm\Delta F$ and so have a partially discrete nature despite their analog origins. Later consideration with quantified justification (see Subsection 6.3), will therefore be given to the possibility of whether the above phase modulations have the capacity to resonantly influence the complex high-order phase modulations upon which the central nervous system's electrical impulse encoding appears to be based (as per [18] and as summarised in Section 4).

6. COMMENCING POSTULATE AND ENSUING HYPOTHESIS

The framework components of a to-be-formed hypothesis have now been established. This Section links these components to provide a justified hypothesis for a CFS mechanism, targeted action upon which (as per Section 7) has, for the presented Case Study, recently coincided with seemed recovery initiation (or at least quantifiable relief) 29 years after CFS onset.

6.1 POSTULATE

A commencing postulate for the encompassing hypothesis is as follows:

Postulate

For the $\Delta\phi_c$ within high-order phase encoding of neural electrical impulses, linear mapping via the transformation $\Delta\phi_c/5 \rightarrow z \rightarrow Z$ to certain elements such as noble gases (suggestive of elementally-proportional quantised neural processes), can be extended to other elements. Extension to such other elements involves the reverse mapping of Z to $\Delta\phi_c$, which also allows the further prediction of corresponding $\bar{\alpha}_{\Delta\phi}$ values via the interpolation of (1).

6.2 EARLY QUANTUM INSIGHTS ARISING FROM POSTULATE

The following early quantum insights for now simply set the scene for results to follow and are somewhat speculative. The primary post-treatment quantum results presented later in Subsection 8.1 do not rely on the element linkages made here (but rather just on the overall sense as reflected in the hypothesis of Subsection 6.3).

The Case Study’s Oligo scan results (figure 2), showing P and B as consistently, markedly, and unusually, having the respective lowest and highest relative levels of 21 reported elements within the scans’ mineral test report, leads one to consider, in an exploratory manner, the places held by these two elements within the neural phase encoding parabola of figure 3. Potential quantum remarkableness lies with the fact that a bodily disposition presents with a P-associated "state" (critical for energy production) having the lowest relative "occupancy" of all 21 elements, and a B-associated state having the highest relative occupancy, with B also associated with the parabola minimum (of figure 3) which could be envisaged as some neural quantum state of minimum energy. In which case, it could be said that the lowest energy state has the highest relative occupancy for the CFS sufferer, and so perhaps suggestive of some kind of *excitational transition or therapeutic deliverance to a higher energy state being required for a return to good health.*

Reversal of the $\Delta\phi_c/5 \rightarrow z \rightarrow Z$ transformation (reverse mapping) for P ($Z = 15$) yields a predicted $\Delta\phi_c = 75^\circ$, with (1) in turn predicting a corresponding $\alpha_{\Delta\phi} = 0.663 \pm 0.012^\circ$ (95% CI), which may also be expressed as $\bar{\alpha}_{\Delta\phi} = 2/3^\circ$ to within 0.5% alignment. Predicted $\Delta\phi_c$ and $\bar{\alpha}_{\Delta\phi}$ values for an individual element from this point will carry a subscript indicative of the element (e.g., $\Delta\phi_p = 75^\circ$ and $\bar{\alpha}_p = 0.663 \pm 0.012^\circ$ for P), which is also appropriate since $\Delta\phi$ clustering, as suggested by the original "c" subscript and explored in [18], is not a present focus. Also, while $\bar{\alpha}_{\Delta\phi}$ values are not further addressed within this early quantum insights Subsection, they are similarly calculated and presented in a unified manner for other elements later.

Following the same reverse mapping modus operandi for B gives $\Delta\phi_B = 25^\circ$, and a subsequent $\Delta\phi_B:\Delta\phi_P$ ratio of 1:3 (which is naturally reflected by the elements’ Z values). In isolation this ratio is arguably unremarkable (although in the context of [18] and its reported ratio-based governance of neural impulse encoding for which 1:3 is a key ratio, perhaps the finding is singularly interesting for a CFS Case Study in which the two elements markedly stand out). Regardless, remarkable status appears reinstated when other elements of interest from the Oligo scan results, namely Zn and Ca, are similarly included alongside P and B. The bases of collective consideration for this quartet of elements within an early quantum insights exploration are summarised by table 2:

Table 2. Quartet element selection bases for the specified reverse mapping analysis leading to possible quantum insights.

Element	Bases for quartet element selection
P	<ul style="list-style-type: none"> Consistently, markedly and unusually displays the <i>lowest</i> relative Oligo scan level out of 21 considered elements. Fundamental role in energy production (e.g., as the basis of ATP). Second most abundant mineral by weight in the human body. Present in every cell.
B	<ul style="list-style-type: none"> Consistently, markedly and unusually displays the <i>highest</i> relative Oligo scan level out of 21 considered elements. Likely necessary component for the formation of life due to a RNA synthesis role. Associates with the parabola minimum in figure 3. Arguably one of the least essential trace elements in terms of bodily function (though its "boring tag" is changing, having for example a known synergy with Ca).
Zn	<ul style="list-style-type: none"> Consistently one of the lowest relative Oligo scan levels out of 21 considered elements. Independently identified by clinical consultants as a primary deficiency to address following Oligo scans. Essential immune system and wound healing roles (sometimes prescribed during viral recovery periods), and in general is quintessentially recognisable as essential for good health. Second most abundant trace mineral after Fe in the human body. A known synergy exists with P.
Ca	<ul style="list-style-type: none"> Consistently one of the few Oligo scan levels in the normal plus range. Most abundant mineral by weight in the human body due to skeletal mineralisation. Key role in muscle contraction (see Subsection 2.4.1 footnote). Key role in cardiac action potential generation and cardiac rhythm maintenance (and thus body clock homeostasis). Key role in cellular signalling/communication [29]. Quintessentially recognisable as essential for good health. Known synergies exist with P, as well as with B.

The predicted $\Delta\phi$ values for P, B, Zn and Ca, when superimposed upon the governing parabola of neural phase encoding, yields figure 4. As graphically highlighted by figure 4, P, Ca and Zn all have associated $\Delta\phi$ values that are integer multiples of B’s value (i.e., of the parabola minimum). Accordingly, the ratios $\Delta\phi_B:\Delta\phi_{Ca}$, $\Delta\phi_P:\Delta\phi_{Zn}$ and $\Delta\phi_B:\Delta\phi_{Zn}$ are 1:4, 1:2 and 1:6 respectively, with $\Delta\phi_B:\Delta\phi_P = 1:3$ previously identified. These findings may imply the presence of some possible quantum connectedness based on integer multiplicity and symmetry. Hence, for the CFS Case Study at hand for which it is suggested that a B-associated quantum neural state is being preferentially occupied over a P-associated quantum neural state, other preferential occupancies (e.g., Ca-associated quantum neural state) might also be indicated.

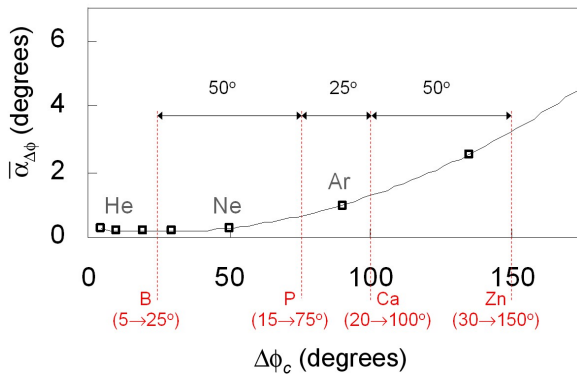


FIGURE 4. $\Delta\phi$ ($\equiv \Delta\phi_c$) values predicted by reverse mapping for B, P, Ca and Zn, and considered as "quantum states" when superimposed upon the governing parabola of neural phase encoding (figure 3).

From the above, ratios such as B:P, B:Zn, B:(P×Zn) and (B×Ca):(P×Zn), based on elemental levels from Oligo or other such scans, may be worthy to explore as possible personal clinical indicators during recovery from long-term (>20 years) CFS. Analysis of these ratios is given later in Subsection 8.2. The possibility of extension to other combinatory indicial personal ratios should not be excluded, while the appropriateness and sensitivity of such indices for shorter CFS durations (i.e., for some other individuals) is left for future consideration.

Finally for this early quantum insights exploration, the spacings of the so-called neural states in figure 4 are analogously mindful of quantum mirror symmetries associated with states of phenomena such as spin-up versus spin-down and matter versus antimatter, and also seemingly consistent with mirror symmetries identified in [18]. However, while Ca inclusion in the above analysis is justified by table 2, its inclusion may be considered convenient given its normal plus (green) level in figure 2. Hence, the mirror symmetry insight is especially tentative. Nonetheless, interest in the quantum-like forms surrounding figure 4 is not diminished if only P, B and Zn are retained, with 1:3:6 ratios and their subsequent symmetries remaining for corresponding $\Delta\phi$ values.

6.3 HYPOTHESIS

The present article’s hypothesis can now be stated and is motivated by the question of: why for the CFS Case Study are the relative occupancies of quantum neural states seemingly "out of kilter". The hypothesis, as partially alluded to within Section 5, is as follows:

Hypothesis

For a minority of persons and in certain circumstances, constant exposure to the modern RF ether, which is becoming increasingly crowded, may compete with the complex phase

oscillations and encodings of neural processes. This competition may not always be completely tolerated, especially (but not just) by those already in compromised states of well-being (e.g., recovering from a virus with neurological impact). More specifically, phase oscillations within the modern RF ether may correspond with element $\Delta\phi$ or $\bar{\alpha}_{\Delta\phi}$ values calculated in accordance with the commencing postulate. Removal of the described competition, combined with positive neural stimulation, might aid in illnesses such as CFS (e.g., via neural rewiring facilitation and activation of key element utilisation, within the confines of element availability).

Clearly, many over several decades have raised concerns over exposure to the modern ether (some in rather eccentric or extreme detrimental ways, and others in more measured ways), and the area of discussion is likely to remain controversial for some time. What is original about the present hypothesis is its ability for justification by quantified results that stem from its highly specific aspects. For now, justification commences with added specificity surrounding RF-neural interaction possibility, as given by Subsections 6.3.1 and 6.3.2. However, before visiting these Subsections it should be reemphasised that the present article is not alarmist about modern ether exposure and, as per Subsection 5.1, holds that society’s exposure should follow the guidelines of stated governing authorities.

6.3.1 FM INTERACTION JUSTIFICATION: SPECIFIC

As per Subsection 5.2, in-practice modulation within FM transmissions is more complex than the simple artificial sinusoidal modulation of (2), and involves the carrier wave still swinging in and out of phase with f_c over multiple cycles, but in a more irregular manner. However, when further visualising a RF wavelength permeating the body at some instant, in-practice modulation remains relatively simple from the overall perspective of the carrier wave being modulated within the limits of $f_c \pm \Delta F$, since this represents an effective phase modulation of $\varphi_{eff} = \pm \Delta F / f_c$ fraction of a complete phase cycle (2π radians or 360°). Typical f_c values fall between 88 to 108 MHz for conventional FM radio (with bands above and below this range for television), and some typical ΔF values are 75, 50, 25, 5, 2 kHz. Thus, an example of $f_c = 100$ MHz, $\Delta F = 75$ kHz corresponds to $\varphi_{eff} = 0.27^\circ$.

The above φ_{eff} value may be relevant since seven of the ten Families of neural phase encoding identified in [18] possess $\bar{\alpha}_{\Delta\phi}$ values in the same vicinity (i.e., between 0 and 1.0°), and it is easy to generate a host of other φ_{eff} values in this vicinity when considering other ΔF and f_c combinations (which also arise from other f_c stations spaced by 100 kHz or similar). Hence, while FM does not directly apply deliberate and specific phase encoding as found within modern digital communications that employ techniques such as phase-shift keying, the alignment between φ_{eff} and $\bar{\alpha}_{\Delta\phi}$ means that some resonant interaction may be possible.

6.3.2 FM INTERACTION JUSTIFICATION: GENERAL

Discrete Phase Noise Effect

As per the brief comment of Subsection 5.2, the phase modulation described by (2b) is expected to bring about a noise effect of discrete side lobes (ordinarily unwanted but digitally utilised in [19]) within a station's bandwidth, which can produce phase oscillations potentially capable of some form of neural phase interference.

Critical kHz Range

The fact that ΔF values are in the kHz range itself may raise the possibility of neural interaction, since the frequencies of music, speech, and audible sound in general, are also in the kHz range (up to ultrasound at 20 kHz). Viz., a multitude of modulations within the $f_c \pm \Delta F$ bandwidth (not the formal definition of bandwidth), and even "beat"-like phenomena between transmissions from different stations, will fall in the audible kHz range. Of course not being sound waves there is no direct audibility, but sound waves at these frequencies are anatomically and physiologically converted into biological electromagnetic signals that are representative of the frequencies, and so it is reasonable to consider the possibility of FM signals in the "critical kHz range" having occasional subtle indirect interaction ability. As previously stated, over the decades several have raised concerns over possible effects of the modern ether, and so the observation here likely overlaps with those of the past.

Lessons from Kindred Ocean Mammals

Within [18] it was revealed that some communication processes of sperm and beluga whales involve simple common fractions that were also identified within the complexities of high-order phase encodings of neural impulses within the human brain. And so it seems that humans have even more in common with such majestic creatures (e.g., than simply being highly intelligent mammals with sophisticated social structures), which as a generalisation will be unsurprising to many.

With the above commonality in mind, the reasons behind the heart-wrenching sight of large pods of these intelligent mammals beaching themselves largely remain a mystery, with the largest recorded beaching in modern history involving approximately 1000 whales upon the Chatham Islands, a New Zealand Territory in the Pacific Ocean, and occurring in 1918 (15 years after Marconi sent the first practical commercial radio message from Massachusetts to England). There are multiple believed reasons behind beachings and some of these are attributed to temporary corruption and confusion within the whales' internal navigation due to interference from electromagnetic field changes, including those brought about by solar flares. This evidence-based (at least in some cases) electromagnetic attribution is generally accepted without major controversy. Hence, a suggestion that the modern ether can affect humans, not at the same acutely obvious

level but in some generally inert or less obvious way, should also remain a possibility amidst calm. After all, in the early years of CFS just a few decades ago, the condition was unfairly branded as "yuppy flu", suggesting modern lifestyle and environment, particularly a technological environment, were contributing factors.

The modern ether is such a complex and condensed amalgamation of so many encrypted signals that it would certainly be deafening, confusing and unbearable if we could actually "hear" the ether as constant background noise (indeed it would have to be many levels worse than being in a crowded room of several loud conversations). Luckily we cannot "hear" the modern ether in this way. However, given that in some respects we are electromagnetic beings, it is again reasonable to suggest that the human brain might possibly be sensitive, in the slightest of ways, to the modern ether (especially older brains without the same generative/compensatory ability of a young, developing brain).

7. "QUANTUM TREATMENT" APPROACH

Seemed recovery initiation for 29 year duration CFS coincided with the completion of an informal "quantum treatment" approach applied in two stages, as outlined below. Since the approach represents an individual's unqualified, self-directed undertaking, it requires refinement and testing within a future controlled formalised study in order to validate any attached claim or finding. Also, the reported recovery could alternatively be explained by coincidence, placebo, or individual responsiveness unhelpful to others (just as other alternative treatment approaches can be highly beneficial to some but not the majority). No attempt should be made to replicate or expand upon the approach outside of a controlled formal study, especially since several possible contraindications exist as identified in Subsection 7.1.

7.1 QUANTUM TREATMENT STAGE 1

Duration

A one hour session undertaken two or (mostly) three times per day, for a period of 23 days.

Regime

Each one hour session consisted of meditation/relaxation within a Faraday-type shielding cage (referred to as a Faraday cage from this point forward), listening to soft classical music (Mozart) lying mostly supine. Since the Faraday cage was not air conditioned, several ice and cold packs were available and utilised as required (i.e., depending on the temperature of the day) to ensure a comfortably cool environment.

Faraday Cage Construction

The Faraday cage was constructed from five sheets of 1200 × 2400 Al (5005 H34 alloy), three sheets being 0.8 mm thick, one being 0.6 mm thick, and one being 1.0 mm thick.

The dimensions of the resulting Faraday cage, with over 95% usage of the available Al, were approximately $1920 \times 1430 \times 700$ mm to allow the housing of a double bed size mattress (figure 5). The Al grade, and range of sheet thickness utilised, were chosen on the basis of: RF attenuation effectiveness, availability, and cost minimisation with the overall cost being approximately \$300 AUD (including Al rivets and L-shaped angle line edging for the cage's opening that seats a removable lid). The usage of the different sheet thicknesses was however somewhat strategic (e.g., with the 1.0 mm sheet being partially used within the cage base and the remainder for the removable lid).



FIGURE 5. Various perspectives of a Faraday-type shielding cage housing a double bed size mattress, with and without removable lid.

Demonstrating the informal, homemade credentials of this latest CFS alleviation effort, functional testing of the Faraday cage simply involved ensuring that a standard non-digital AM/FM radio and cell phone (both placed internally to the cage) remained disconnected reception-wise. It was also ensured through pulse oximetry that blood oxygen saturation percentage, or SpO₂ levels, were not observably affected for a personal enclosure duration of 1.5 hours.

Regime Rationale

The rationale behind shielding against RF exposure is explained within Subsections 5.1 and 6.3. The rationale behind the (mostly) thrice daily approach in part comes from the impracticality of whole-house, or even whole-room, Faraday cage constructions, which are clearly incongruous for an intended inexpensive and simple homemade trial. However, the thrice daily approach was also influenced by the success that some (by no means the majority) have had with other sessional (per-day) therapy regimes (e.g., neural rewiring and cryogenic therapy in the form of ice baths). Such success stories *may* indicate that whatever system/neural reboot is needed for CFS recovery, it can be achieved on an hours-per-day therapy basis.

The ice/cold pack application was with the intention of being comfortable not "torturous", so as to provide a conducive meditation/relaxation environment (which was indeed subjectively the case). The ice/cold pack application was also inspired by the quantum-based suggestion of Subsection 6.2 that CFS might be linked to a minimum quantum neural state⁶ associated with the turning-point of figure 3, and so might positively respond to some kind of targeted "excitation" to a healthier quantum neural state. An assumption was made that elevated core body temperature should be avoided for such positive excitation, however because the applied therapy regime aimed to be relatively passive and comfortable, significant core body temperature reduction was avoided.

The classical music component was included to enhance relaxation, and was also motivated by the neural phase encoding connectedness with music theory as found in [18] and the copious formal studies demonstrating the neuro-benefits of music therapy (as briefly introduction in [18]).

Contraindication Examples

Some perceived risks of the above-described treatment approach include: adverse reactions to a confined space including for asthmatics due to reduced airflow; falling asleep in a confined airflow space; working with "sharps" in the form of sheet metal and metal filings; Al exposure; instability of a relatively heavy assembly if not securely constructed; ice burns and/or adverse blood circulatory effects due to ice/cold pack application.

7.2 QUANTUM TREATMENT STAGE 2

Progress results following the 23 day Stage 1 quantum treatment protocol, and based on an Oligo re-scan (December 7), displayed modestly encouraging indicators as outlined within the next Quantum Results Section. However, an unexpected outcome of the re-scan was a seemingly appreciable Al increase within its report's heavy metal test component. The percentage Al increase in relation to the average of the January 19 and August 16

⁶Or maximum state depending on one's perspective (i.e., minimum available energy, maximum immune system response, and so on...)

scans was 37%. Since percentage increase can be misleading without consideration of distribution statistics such as standard deviation, providing a less dramatic but still commanding comparison was the re-scan report's qualitative AI level description of "high plus", having been elevated from "high" and "high minus" respectively in relation to the pre-treatment scans.

While the above unexpected outcome was certainly unwanted and demonstrates how adverse outcomes can result outside of a formally controlled study, as per the Oligo scan repeatability comment of Subsection 2.4.3, here again one cannot help but be impressed, this time in relation to scan sensitivity. That is, the re-scan was seemingly sensitive to the activities of construction of, and/or meditation/relaxation within, an AI Faraday cage over several weeks. Gloves were worn for most (but not all) stages of construction and hands were otherwise washed post any construction activity. Hence, the adverse outcome might be explained by carbonic acid, from carbon dioxide build-up within the confined cage, reacting with (vapourising) AI surfaces in relatively early stages of oxidation (which begins immediately upon surface exposure to the atmosphere).

Due to the adverse AI outcome and competing external factors, the treatment trial was suspended for several weeks. During this time-out the internal surfaces of the Faraday cage were sealed with several coatings of extremely low volatile organic compound (VOC) interior house paint marketed for its gentleness in relation to fumes and breathability.

A parallel decision was also made to modify the Faraday cage to increase its ventilation, thereby allowing internal sleeping at nights (so as to possibly increase treatment effectiveness due to body repair and immune system activity that occur during sleep). Accordingly, a duplicate lid was fabricated with over 1100×1 mm diameter drill holes spaced in a 3 cm square grid arrangement to give an overall (modest) ventilation area of approximately 9 cm^2 . With this night-use lid in place, pulse oximetry percentage SpO_2 levels were not observably affected for a personal enclosure duration of at least 4.5 hours. Enclosure testing beyond this time was not required since night sleeping was intended for up to 4 hours only (representing at least half of the night's sleep).

Approximately 11.5 weeks after the completion of the Stage 1 trial, the Stage 2 trial, involving a daily 60 to 70 minute meditation/relaxation session (one only) and night sleeping for up to 4 hours (approximately 3 hours on average), commenced for a duration of 32 days. After settling into this Stage 2 routine, its sleeping period was scheduled for the "second half" of the night so as to wake up to a new day from the Faraday cage. An Oligo re-scan for the Stage 2 trial was undertaken on March 30, 2022 at a third independent clinic.

8. QUANTUM RESULTS AND DISCUSSION

The following results are from a medical/quantum physicist's perspective without qualifications in nutrition. Thus, nutritional advice is not intended and nor should it be taken from any surrounding discussion.

8.1 PRIMARY QUANTUM ANALYSIS

8.1.1 OVERVIEW (NON-QUANTUM)

Subjective feelings of diarised symptom improvement following Stage 2 treatment, rated as modest, moderate or appreciable and which generally improved upon Stage 1 outcomes, include:

- Reduction in muscle aches (appreciable).
- Reduction in primary governing fatigue (modest-to-moderate).
- Increase in exercise endurance ability (moderate).
- Increase in mental clarity and resilience to mental exertion (moderate).
- Improved (less broken) sleep (modest-to-moderate).

The reduction in muscle aches was particularly noticeable even midway through Stage 1. Before treatment commencement, the continuity of exercise was not possible due to what felt like frequent and wide-spread "micro muscle tears", not just during exercise but upon everyday movements (possibly consistent with the clinical diagnosis of Subsection 2.4.1). By the end of Stage 2, such muscular injury and discomfort had significantly abated allowing a return to exercise continuity and with increased endurance.

While the above subjective feelings of improvement are encouraging, it is recognised that the improvements could simply be attributable to the benefits of prolonged meditation/relaxation which had never before been undertaken for periods comparable to those of the treatment.

Interesting and more quantifiable preliminary outcomes are observed when the 21 element listing of the post-treatment Oligo scans (of December 7, 2021 for Stage 1 and March 30, 2022 for Stage 2) are re-ordered based on the percentage change of element level, as compared to the average of the original January 19 and August 16 pre-treatment 2021 scans (the four scans in chronological order will be referred to as Scans 1, 2, 3 and 4). In descending order of percentage change (i.e., ranked from largest positive change down), table 3 gives the top four elements of scan 4⁷. Other than a slight reordering of the elements (but with Co still remaining in 1st position), the elements identified by table 3 do not change if Scan 4 is compared only against the most recent pre-treatment Scan 2 (this

⁷Does not include Se which is omitted from the 21 element analysis due to its marked transient nature between all four Oligo scans. However, Se is considered an essential antioxidant and reduces in level with brain aging such that level targeting through strategies such as dietary supplementation with exercise may reverse memory loss (e.g. in Alzheimer's disease [30]). Hence, significance of the transient observation should not be discounted.

outcome is expected due to the consistency between Scans 1 and 2). Also, a similar analysis for Scan 3 identifies the same elements (with a change of rank order) with reduced percentage change, indicating that the Scan 4 outcomes of table 3 are not random (i.e., not one-off for the day of the scan) but the result of progressive change.

Note that no vitamin/mineral supplements were regularly or sporadically taken during the months leading up to Scans 3 and 4 and similarly no changes in dietary or other relevant habits were introduced during that same period (with a diet consisting of drinking purified non-fluoridated water as standard, and toothpaste brand/type remaining constant).

Table 3. Elements with the largest positive percentage change in level (bracketed value) when comparing post-treatment Oligo Scan 4 with the average values of pre-treatment Scans 1 and 2.

Ranking [#]	1	2	3	4
Element	Co (+15.8)	Li (+14.8)	P (+14.1)	F (+13.4)

[#]Rankings are simple in that the percentage changes that govern rank do not consider the standard deviations of element level population distributions.

The four elements identified by table 3, which do not all commence from an obviously low base level, are of interest because of the following possibly pertinent facts:

- The first-ranked element in table 3, Co, plays critical neurophysiological roles and, particularly in the form of vitamin B12 (cyanocobalamin), enhances nerve repair, improves functional recovery after brain injury, and is central to the production of haemoglobin [31,32]. These roles partly stem from being an integral component of a biochemical reaction (transmethylation) that is essential to myelin sheath protein production [31]. Also, upon linear mapping Co is identified in [18] as representing one of the ten Families of neural phase encoding.
- The second-ranked element in table 3, Li, is known to (i) stimulate the proliferation of stem cells, including neural stem cells; (ii) increase the concentrations of neural markers (n-acetyl-aspartate and myoinositol) in the brain; (iii) have a protective effect towards neurons; and (iv) increase brain cell density and volume in patients with bipolar disorder (has long been used by clinicians to treat manic depression) [33].
- The third-ranked element in table 3, P, is a key element identified by the present article as having possible quantum significance (see figure 4 and surrounding commentary), and naturally is key to energy production as per Section 3.
- For the fourth-ranked element in table 3, F, a possibly intriguing aside (for some), is that fluorite crystal is often associated with focus, mental clarity and peace of mind within metaphysical practices.

- Of the 21 elements, Co, Li, P and F are the *four most magnetically/electromagnetically relevant* in terms of quantities such as gyromagnetic ratio, γ , nuclear spin quantum number, I , and spin magnetic dipole moment, μ , as well as in terms of ferromagnetism (elaborated upon with brief explanation of quantities within the next Primary Quantum Results Subsection 8.1.2).

Note that the neurotoxic effects, at adversely elevated levels, of some of the trace elements identified above are acknowledged but not expanded upon within continuing discussion.

Another interesting feature of Scans 3 and 4 is the progressive decline in Mg level, with a substantial -36.1% and -40.8% change at Scans 3 and 4 respectively (again as compared to the average of Scans 1 and 2 which is implied from this point unless otherwise stated). Also, despite the progressive +14.1% increase in P as displayed by table 3, Scan 4 still shows P levels in the low minus (red) region, such was its extremely low commencing base level, and the originally low Zn and Cr levels slipped further backwards in Scan 4 to also join P in the low minus region. More specifically, the overall declines of Zn and Cr at Scan 4 are -5.2% and -5.6% respectively, with Cr actually joining P in the low minus region as of Scan 3.

Understandably, some may express concern at the above Mg, Zn and Cr outcomes (if physiologically legitimate), particularly for Mg given its importance for muscles undergoing exercise, thereby spelling a need for treatment approach avoidance. In the fullness of time that position may prove correct. However, for now a contrary positive position is given consideration. The fact that of the scans' 21 elements, Mg undergoes a substantial and the largest percentage decline, and this decline coincides with a considerable subjective reduction in muscular symptoms, appears to support that the removal of modern ether influences, combined with neural stimulation, had some physiological effect, albeit an unexpected effect. And so one might ask questions such as, does the decline reflect:

- *Muscular uptake of Mg?*
- *Temporary preferential recovery, at the expense of Mg, of the identified most magnetically relevant elements?*

Moreover, long-term disruption of element uptake and metabolic processes may negate body homeostasis and be unpredictably reflected within attempted restorative changes and negative feedback processes (including within the Krebs cycle as per Subsection 2.4.1, and as the body expends energy to maintain affected magnetically relevant elements). Similarly, the removal of said disruption may result in an unexpectedly involved path back to the equilibrium of homeostasis. The Mg result should not however be considered in isolation (i.e., Ca, one of the few elements at a relatively high but still normal pre-treatment level, also underwent progressive decline as discussed shortly in Subsection 8.2).

8.1.2 PRIMARY QUANTUM RESULTS

It is mathematically revealing to collate results of the seven elements with marked outcomes, as identified in the previous Subsection (Co, Li, P, F, Mg, Zn and Cr). The collation of these elements is summarised by table 4 (and see its footnote for the basis of extra Mo inclusion).

Table 4 is mathematically fascinating since for all of the elements: (i) **Z values are integer (n) multiples of 3**;

- (ii) elements with a *positive* change (Co, Li, P and F) display *odd* values of *n*, while elements with a *negative* change (Mg, Zn, Cr, and Mo) display *even* values for *n*;
- (iii) $\Delta\phi$ values are integer or half-integer (*m*) multiples of 30° ; and (iv) elements with a *positive* change display *half-integer* multiples of *m*, while elements with a *negative* change display *integer* multiples of *m*.

Table 4. Summary of elements with the most notable percentage change in level (bracketed) when comparing post-treatment Oligo Scan 4 with the average values of pre-treatment Scans 1 and 2. Element Z values are written as integer, *n*, multiples of 3, and $\Delta\phi$ values predicted by reverse mapping of Z are written as *m* multiples of 30° , where *m* is an integer or integer multiple of a common fraction. Reverse-mapping-predicted $\bar{\alpha}_{\Delta\phi}$ values are given with uncertainties at 95% CI. Median $\bar{\alpha}_{\Delta\phi}$ values that fall within 0.5% of, or approximate to, a nominal integer, or integer multiple of a fraction ($\frac{1}{2}$ or $\frac{1}{4}$), are given in the two right-most columns (with the percentage deviation from nominal bracketed). The rightmost inset, for comparison of form, displays the fine structure energy levels of hydrogen based on a rotational kinetic energy extension to Bohr's model [34].

Basis for element inclusion	Element (% change)	Z	n (Z = n×3)	$\Delta\phi$ (degrees)	m ($\Delta\phi = m \times 30^\circ$)	Model $\bar{\alpha}_{\Delta\phi}$ (degrees)	Nominal $\bar{\alpha}_{\Delta\phi}$ (% departure)
Largest % increase	Co (+15.8)	27	9	135	4½	2.5550 ± 0.0241	≈ $\frac{5}{2}$ (+2.2)
	Li (+14.8)	3	1	15	½	0.1948 ± 0.0037	≈ $\frac{1}{5}$ (-2.6)
	P (+14.1)	15	5	75	2½	0.6631 ± 0.0121	≈ $\frac{2}{3}$ (-0.53)
	F (+13.4)	9	3	45	1½	0.2510 ± 0.0075	≈ $\frac{1}{4}$ (+0.41)
Largest % decrease	Mg (-40.8)	12	4	60	2	0.4126 ± 0.0097	≈ $\frac{2}{5}$ (-3.1)
Low minus or "red" level#	Zn (-5.2)	30	10	150	5	3.2504 ± 0.0277	≈ $3\frac{1}{4}$ (+0.01)
	Cr (-5.6)	24	8	120	4	1.9486 ± 0.0208	≈ 2 (-2.6)
	Mo (-14.9)	42	14	210	7	6.9218 ± 0.0441	≈ 7 (-1.1)

#P also qualifies for the low minus category. Mo is shaded since it displays the lowest level of all elements after P, Zn, and Cr, falling just above the low minus threshold.

TABLE 1
COMPARISON OF PREDICTED FINE STRUCTURE ENERGY SHIFTS, $C \times \Delta RKE_n$, WITH DIRAC THEORY FOR SELECTED LEVELS

Level	C	$C \times \Delta RKE_n$ ($\times 10^4$ eV)	Dirac theory ($\times 10^4$ eV)	Difference (%)
1S	1	1.812	1.8101	0.10
2P	1	0.1132	0.11283	0.33
2S	5	0.5662	0.56537	0.15
3D	1	0.02237	0.022317	0.24
3P	3	0.06710	0.066951	0.22
3S	9	0.2013	0.20085	0.22

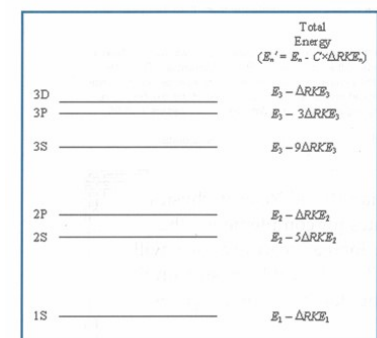


Fig. 2 The 1S, 2S, 2P, 3S, 3P and 3D energy levels predicted by the extended Bohr theory.

The probability of randomly selecting seven elements, with the identified Z multiplicity of 3, from the defined Oligo set is $p = 0.0001$ (and $p < 0.00001$ with Mo inclusion). Even if table 4 construction is considered selective (which to a degree it is since for example the number of elements in each table category differ), the probability of chance occurrence is still considerably low. Furthermore, even though results independence cannot be claimed for established reasons, the findings are based on consistent clinical reports independently obtained from three separate health providers. Findings could not have been foreseen (short of deliberately removing elements such as P and Zn for an extended time from one's diet etc.).

The fascinating (i) to (iv) outcomes above actually display many quantum mechanical characteristics, some of which include:

- Categorisations based on positive versus negative, even versus odd, integer versus half-integer (mindful of quantum properties such as charge, parity and spin).
- In regards to nuclear spin, the increasing elements of Co, Li, P and F have half-integer *I* values ($I = 7/2, 3/2, 1/2$ and $1/2$ respectively with magnitudes in table order), while the decreasing elements of Mg, Zn, Cr and Mo have $I = 0$.
- The $\Delta\phi = m \times 30^\circ$ multiplicity is interesting since symmetrical occurrences involving 30° (and therefore 60°) govern the quantum properties of elementary particles, for which properties such as charge, spin, strangeness, etc. can be geometrically arranged in various triangular and hexagonal arrays in which such angles are inherent (e.g., hadron arrangement within SU3 group symmetry).

- The $\Delta\phi$ values can in fact be written as multiples of any angle (i.e., not just 30°) with a corresponding multiplicative change in m (such as $\Delta\phi = m' \times 45^\circ$, where m' is an integer, or integer multiple of $1/3$, and $\Delta\phi = m'' \times 90^\circ$, where m'' is an integer multiple of $1/6$). For the latter 90° case (for which m'' values in the elemental order of table 4 are $9/6, 1/6, 5/6, 3/6, 4/6, 10/6, 8/6$ and $14/6$), it might *loosely* be said that the overall neuro-quantum state (or function) at the time of Scan 4 is formed from a set of *orthogonal* basis states (or functions), which is a most quantum-like scenario.
- Another interesting quantum mechanical characteristic of table 4 comes from comparison with an extension to Bohr's model of atomic hydrogen [34] (while Bohr's model and this extension are semi-quantum due to their classical aspects, they still arguably provide useful physical insights amidst the inherent restrictions of classicality). The extension includes integer, C , multiples of an analytically derived electron rotational kinetic energy (ΔRKE) term and predicts the fine structure energy shifts of electron orbits to high accuracies comparable to Dirac's relativistic treatment. The ΔRKE term is given by:

$$\Delta RKE_n = \frac{\pi m^2 r_e Z^3 e^6}{16 \epsilon_0^3 h^4 n^4}, \quad (3)$$

where m is electron mass⁸, r_e is electron radius, e is electron charge magnitude, ϵ_0 is the permittivity of free space, h is planck's constant, and n is an integer signifying the principal orbit (i.e., is a principal quantum number). Clearly, the m and n in (3) differ from the m and n notation used within table 4, however the original notation of [34] is retained since ambiguity is unlikely and the notation is archetypal of atomic physics and Bohr's model.

A results table from the 2003 *Physics in Canada* publication of the extended model [34], showing the fine structure energy shifts of various orbits in terms of C multiples of ΔRKE_n , is given as an inset to table 4. The tables are presented side-by-side for comparison purposes since the n values for elements with a positive increase in table 4 (i.e., $n = 1, 3, 5$ and 9), take the same integer values of C in the table inset. The comparison finding is perhaps representative of the fact that quantum mechanical geometric symmetries (e.g., within energy level diagrams) are known to approximately and proportionally reoccur across many atomic scales. This comparison might be further explained by the fact that the $C = 1, 3, 5$ and 9 fine structure differentiation represents preferred lowest or conventional states of hydrogen, and Case Study treatment outcomes seem to indicate a progression towards increased occupancy of some preferred lower neuro-quantum states.

⁸Accuracy is enhanced by substituting the reduced mass expression, $mM/(m + M)$ for m , where M is the mass of the hydrogen nucleus.

The Co, Li, P and F description as "most magnetically relevant" in Subsection 8.1.1, and their noting within a recent dot point of having half-integer I (with the decreasing elements of table 4 conversely having $I = 0$), indeed warrant further discussion. The elements are described as most magnetically relevant since F, P and Li appear highest behind H in tabulations (e.g., within MRI) of biological magnetically active elements of abundance and with high γ (recall H is also associated with one of the primary Families of neural phase encoding in [18]). In MRI-type scenarios, γ sets the precession frequency for a given applied magnetic field (as raised in Subsection 5.1) and classically is a measure of how much magnetic effect one gets from a spinning charged particle ($\gamma = \mu/S$ where S is intrinsic spin angular momentum which I parameterises). The γ values of F, P and Li are 40.1, 17.2 and 16.5 MHz/T respectively, compared to 42.6 MHz/T for H (the nuclear magnetic sensitivity of Co is slightly higher than that of Li).

It is also intriguing that Co is one of only three ferromagnetic (at room temperature) elements of biological relevance, the others being Fe ($I = 0$) and Ni ($I = 3/2$), with the trio of transition metals appearing consecutively within the same row of the periodic table. Ferromagnetism is more concerned with *electron* spin, but nonetheless has effect in the MRI environment (as an ongoing analogy) of RF waves and magnetic fields (e.g., ferromagnetism may cause artefacts due to introduced magnetic field heterogeneities).

It is quite fascinating and potentially telling that the *heavy metal* element with the largest percentage increase is Co's ferromagnetic partner, Ni (see Appendix A), while over several years of CFS blood ferritin levels were above typical range without supplements (see Subsection 2.4.4). Adding further fascination, if not supporting evidence, Cr at the opposite end of table 4 is the only *antiferromagnetic* element. Hence, accumulated evidence is suggestive of modern ether removal combined with neural stimulation having catalysed the uptake of the most magnetically relevant elements (which includes P, the focus of previous Sections), from which one might hypothesise that removal of neural phase interference has initiated a biological recovery or response.

When considering the possibility of modern ether interference effects, the $\Delta\phi$ values of table 4 elements being expressible in terms of landmark Cartesian/polar angles (e.g., $\Delta\phi_{Co} = 90^\circ + 45^\circ$, $\Delta\phi_{Li} = 45^\circ - 30^\circ$, $\Delta\phi_P = 45^\circ + 30^\circ$, $\Delta\phi_F = 45^\circ$, $\Delta\phi_{Mg} = 60^\circ$, $\Delta\phi_{Zn} = 180^\circ - 30^\circ$, $\Delta\phi_{Cr} = 180^\circ - 60^\circ$, $\Delta\phi_{Mo} = 270^\circ - 60^\circ$) is interesting despite some degree of mathematical expectedness. Interest here derives from some phase-shift keying schemes within digital RF communication encoding using such angular values for their phase shifts. Also, $\Delta\phi$ formation about landmark angles here is generally consistent with the radial geometry of neural phase wheels in [18] (see within for phase wheel definition). However, CFS has existed since before the

advent of digital RF communication, and so the interference justification of Subsection 6.3.1 remains a primary justification.

Another interesting observation for table 4 is that $\bar{\alpha}_{\Delta\phi}$ values approximate as integers or simple common fractions. Interest in integer/fractional-integer alignment for $\bar{\alpha}_{\Delta\phi}$ stems from possible connectedness to some quantum process, since such multiplicities are quintessentially characteristic of a range of quantum systems. Interest also stems from possibly providing another avenue for modern ether interference (as explained within Appendix B, wherein Table B1 lists all elements from $Z = 1$ to 63 for which generated median $\bar{\alpha}_{\Delta\phi}$ values fall within 0.5% of some integer, or integer multiple of $\frac{1}{3}$ or $\frac{1}{4}$).

Note that the $\bar{\alpha}_{\Delta\phi}$ values predicted by (1) and given in table 4 and table B1 are taken as falling exactly on the $\bar{\alpha}_{\Delta\phi}$ versus $\Delta\phi_c$ model curve of figure 3, whereas in [18] all Family $\bar{\alpha}_{\Delta\phi}$ values fall slightly off the model curve (as is the norm for most curves-of-best-fit), despite the curve's exceptionally high correlation. In [18] it is assumed with justification that these slight departures or residuals carry quantum significance. While that assumption is still firmly advocated, the present article takes $\bar{\alpha}_{\Delta\phi}$ values as falling exactly on the $\bar{\alpha}_{\Delta\phi}$ versus $\Delta\phi_c$ model curve for convenience (here the same level of high precision analysis is not required for points made), and because both perspectives can readily co-exist and hold quantum significance⁹.

Due to the approximate integer/fractional-integer values of $\bar{\alpha}_{\Delta\phi}$ in table 4, the ratios of these values will also naturally approximate as integers or simple common fractions as per [18] (wherein $\bar{\alpha}_{\Delta\phi}$ values are generally not integers or fractional-integers and are known to higher accuracy, and so the formation of precise ratio values in [18] is more remarkable).

Other quantum mechanical comparisons can be made for table 4 which accounts for most of the relevant body elements with $Z = n \times 3$ (the Oligo scan understandably does not include C, Ar and Kr). However, these comparisons are not pursued here, with other interesting Oligo scan outcomes now preferentially explored.

8.2 PERSONAL QUANTUM INDICES

Subsection 6.2 shared early quantum insights, involving the elements B, Ca, P and Zn, which set the current scene. Within that Subsection the ratios B:P, B:Zn, B:(P×Zn), and (B×Ca):(P×Zn), were proposed as possible personal CFS indices during recovery. Returning for a closer inspection of these elements, it can now be revealed that over the course of Scans 3 and 4, the relatively high values of B and Ca progressively reduced by overall amounts of -14.8 and -15.6% respectively, to the point of B no longer being the

element with the highest level (a quite interesting outcome in the absence of any dietary change or supplement intake).

Table 5 contains the values of these ratios for Scans 1 to 4, with the B:P and (B×Ca):(P×Zn) ratios demonstrating the largest progressive changes of -34% and -51% respectively at Scan 4. Hence, the ratios appear to be sensitive to perceived feelings of CFS improvement, and the progressive declines in B and Ca with increase in P suggest that the quantum scenario speculated in Subsection 6.2 might possibly hold some basis. Of course despite the 14.1% increase in P, the fact that P and Zn levels are in the low minus region at Scan 4 would mean that there is much scope for further recovery and corresponding ratio declines (as per subjective feelings). The slipping backwards of Zn levels mathematically explains why some of the proposed indices appear less sensitive than others at the Scan 4 stage of seemed recovery.

Table 5. Ratios B:P, B:Zn, B:(P×Zn), and (B×Ca):(P×Zn), proposed as possible personal CFS indices, calculated from the elemental values pre-treatment Scans 1 and 2, and post-treatment Scans 3 and 4. The percentage changes (bracketed) are in comparison to the average of the two pre-treatment scans.

Ratio	Scan 1 (19 Jan)	Scan 2 (16 Aug)	Average (pre-treatment)	Scan 3 (7 Dec)	Scan 4 (30 Mar)
B:P	0.0374	0.0346	0.0360	0.0320 (-13)	0.0269 (-34)
B:Zn	0.0303	0.0296	0.0299	0.0270 (-11)	0.0269 (-11)
B:(P×Zn)	0.000329	0.000298	0.000314	0.000281 (-12)	0.000247 (-27)
(B×Ca):(P×Zn)	0.187	0.174	0.181	0.145 (-25)	0.120 (-51)

The in-tissue -15.6% decline for Ca could alone carry important ramifications beyond illnesses like CFS, but on this point especially one should not speculate upon tentative results.

9. CONCLUSIONS, FUTURE DIRECTIONS AND IMPLICATIONS

The many identified quantum characteristics of element level changes for a long-term CFS sufferer in response to modern ether removal and neural stimulation may suggest that electromagnetic environmental factors can have an adverse neurophysiological effect for the susceptible few and that the high-order phase encodings of neural processes are indeed quantum mechanically based.

The quantified explanation as to why the modern ether may have an adverse neurophysiological effect is original and arguably convincing (e.g., partially based upon the phase modulations of FM transmissions overlapping with key $\bar{\alpha}_{\Delta\phi}$ values of neural phase encoding). Also arguably convincing is the fact that in response to modern ether removal, the most magnetically relevant body elements displayed the largest percentage increase in levels. Implications of this outcome may explain why the large majority of people who recover

⁹As an analogy, electron orbits of the principal energy levels of the hydrogen atom carry exact parabolic functionality of significance [18,34], but fine structure energy levels which are perturbed slightly away from the principal levels also carry significance.

from CFS do not fully recover to pre-illness energy levels (i.e., the continuing presence of the modern ether may cause chronic low-level neural phase interference despite some degree of effective neural rewiring or related recovery).

The presented Case Study results may show a system that has begun to heal in response to the applied (in two stages) "quantum treatment" by: an appreciable reduction in muscular discomfort; a modest-to-moderate reduction in primary fatigue; a moderate increase in exercise endurance ability; P levels being on the increase; and marked changes in proposed personal quantum indices. Treatment has continued since the end of the Stage 2 reporting, with further subjective improvements experienced. Over the course of 29 years no other approach has brought any meaningful personal relief and, like all with CFS, the approaches trialled have been numerous.

As advocated throughout, a future controlled formalised study is required to uphold the presented justified hypothesis and its quantum mechanical rationale with tentative findings. If the hypothesis is upheld, then the following final messages ensue:

- One or more of the (in tissue) ratios, B:P, B:Zn, B:(P×Zn), or (B×Ca):(P×Zn), may be useful personal indices for relative monitoring during CFS recovery, especially for long-term CFS sufferers.
- Research into how RF communication approaches can be modified to avoid or reduce the risk of possible subtle adverse neurological health effects (originating from complex neural impulse phase signalling interference) in the susceptible few would be indicated. For the majority such modifications would not be necessary, as per the non-alarmist tone throughout in regards to modern RF ether exposure. As research and understanding progress, similar modifications but in favour of the majestic intelligent mammals of the ocean may also be indicated.
- The complementary use of music therapy can most likely be improved upon, especially given that some neurological illnesses require interventions as invasive as deep brain stimulation. Hence, the replacement of music therapy by a slightly less passive complementary treatment partner (e.g., transcranial magnetic stimulation) may prove more effective whilst also catering for hearing impaired persons involved in any future study.
- A discussion on the potential benefits of regular meditation or quiet time, not just within a space free of distraction, but also within an electromagnetically silent space, is encouraged (which naturally carries over to home/workplace design and daily practices).
- On a more broad philosophical level, if a mostly inert, invisible and widely-considered socially beneficial

phenomenon such as RF atmospheric transmissions can, for a susceptible few, subtly (without known definitive biomarkers) hinder neural recovery or facilitate adverse neurological health effects, what then must be the long-term adverse environmental and health effects of the unfathomable tonnage of toxic pollutants continually pumped and dumped upon our once pristine Earth?

REFERENCES

1. Kim DY, Lee JS, Park SY, Kim SJ, Son CG. 2020 Systematic review of randomized controlled trials for chronic fatigue syndrome/myalgic encephalomyelitis (CFS/ME). *J. Transl. Med.* **18**:7. (<https://doi.org/2010.1186/s12967-019-02196-9>)
2. Brenna E, Araja D, Pheby DFH. 2021 Comparative survey of people with ME/CFS in Italy, Latvia, and the UK: A report on behalf of the Socioeconomics Working Group of the European ME/CFS Research Network (EUROMENE). *Medicina* **57**:300. (<https://doi.org/10.3390/medicina57030300>)
3. Muirhead N, Muirhead J, Lavery G, Marsh B. 2021 Medical School Education on Myalgic Encephalomyelitis. *Medicina* **57**:542. (<https://doi.org/10.3390/medicina57060542>)
4. Action for ME. *What is ME Introduction and Big Survey* [Internet, cited 2021 July 23]. Available from: <https://www.actionforme.org.uk>
5. Kapur N, Webb R. 2016 Suicide risk in people with chronic fatigue syndrome. *Lancet* **387**, 1596-1597. ([https://doi.org/10.1016/S0140-6736\(16\)00270-1](https://doi.org/10.1016/S0140-6736(16)00270-1))
6. Komaroff AL. 2019 Advances in understanding the pathophysiology of ME/CFS. *JAMA* **322**, 499-500. (<https://doi.org/10.1001/jama.2019.8312>)
7. Sandler CX, Lloyd AR. 2020 Chronic fatigue syndrome: Progress and possibilities. *Med. J. Aust.* **212**, 428-433. (<https://doi.org/10.5694/mja2.50553>)
8. Saha AK, Schmidt BR, Wilhelmy J, Nguyen V, Abugherir A, Do JK, Nemat-Gorgani M, Davis RW, Ramasubramanian AK. 2019 Red blood cell deformability is diminished in patients with chronic fatigue syndrome. *Clin. Hemorheol. Microcirc.* **71**, 113-116. (<https://doi.org/10.3233/CH-180469>)
9. Miwa K. 2015 Cardiac dysfunction and orthostatic intolerance in patients with myalgic encephalomyelitis and a small left ventricle. *Heart Vessels* **30**, 484-489. (<https://doi.org/10.1007/s00380-014-0510-y>)
10. Richards RS, Wang L, Jelinek H. 2007 Erythrocyte oxidative damage in chronic fatigue syndrome. *Arch. of Med. Res.* **38**, 94-98. (<https://doi.org/10.1016/j.arcmed.2006.06.008>)
11. Morris G, Maes M. 2014 Mitochondrial dysfunctions in myalgic encephalomyelitis/chronic fatigue syndrome explained by activated immuno-inflammatory, oxidative and nitrosative stress pathways. *Metab. Brain Dis.* **29**, 19-36. (<https://doi.org/10.1007/s11011-013-9435-x>)
12. Marshall M. 2020 COVID-19's lasting misery. *Nature* **585**, 339-341. (<https://doi.org/10.1038/d41586-020-02598-6>)
13. Marshall M. 2020 How COVID-19 can damage the brain. *Nature* **585**, 342-343. (<https://doi.org/10.1038/d41586-020-02599-5>)
14. Basted AC, Marshall LM. 2015 Review of myalgic encephalomyelitis/chronic fatigue syndrome: an evidence-based approach to diagnosis and management by clinicians. *Rev. Environ. Health* **30**, 223-249. (<https://doi.org/10.1515/revh-2015-0026>)
15. Shepherd CB. 2017 PACE trial claims for recovery in myalgic encephalomyelitis/chronic fatigue syndrome – true or false? It's time for an independent review of methodology and results. *J. Health Psychol.* **22**, 1187-1191. (<https://doi.org/10.1177/1359105317703786>)
16. Marshall M. 2021 COVID's toll on small and taste: what scientists know. *Nature* **589**, 342-343. (<https://doi.org/10.1038/d41586-021-000556>)
17. Douaud G, Lee S, Alfaro-Almagro F, Arthofer C, Wang C, McCarthy P, Lange F, Andersson JLR, Griffanti L, Duff E, et al. 2022 SARS-CoV-2 is associated with changes in brain structure in UK Biobank. *Nature*. (<https://doi.org/10.1038/s41586-022-04569-5>)
18. Simeoni RJ. 2021 A new approach to high-order electroencephalogram phase analysis details the mathematical mechanisms of central nervous system impulse encoding. *UNET J. Sci. Soc.* **1**, 1-34. (<https://doi.org/10.52042/UNETJOSS010101>)

19. Simeoni RJ. A discrete oscillator phase noise effect applied within phase-shift keying RF digital signal modulation. In: 9th International Conference on Signal Processing and Communication Systems; 2015 December 14-16; Cairns, Australia. p. 1-9. (<https://doi.org/10.1109/ICSPCS.2015.7391745>)
20. British Broadcasting Corporation. 2013 *The truth about sleep*, Producer England R.
21. British Broadcasting Corporation. 2016 *Medical mavericks: the history of self-experimentation*, Producer Gregory A.
22. Sinclair HM. 1956 Deficiency of essential fatty acids and atherosclerosis, etcetera. *Lancet* **267**, 381-383. ([https://doi.org/10.1016/S0140-6736\(56\)90126-X](https://doi.org/10.1016/S0140-6736(56)90126-X))
23. Sjölin J, Stjernström H, Henneberg S, Hambraeus L, Friman G. 1989 Evaluation of 3-methylhistidine excretion in infection by 1-methylhistidine and the creatine ratios. *Am. J. Clin. Nutr.* **49**, 62-70. (<https://doi.org/10.1093/ajcn/49.1.62>)
24. Sheffield-Moore M, Dillon EL, Randolph KM, Casperson SL, White GR, Jennings K, Rathmacher J, Schuette S, Janghorbani M, Urban RJ, et al. 2014 Isotopic decay of urinary or plasma 3-methylhistidine as a potential biomarker of pathologic skeletal muscle loss. *J. Cachexia Sarcopenia Muscle* **5**, 19-25. (<https://doi.org/10.1007/s13539-013-0117-7>)
25. Juste C, Gerard P. 2021 Cholesterol-to-coprostanol conversion by the gut microbiota: what we know, suspect and ignore. *Microorganisms* **9**:1881. (<https://doi.org/10.3390/microorganisms9091881>)
26. Mutter J. 2011 Is dental amalgam safe for humans? The opinion of the Scientific Committee of the European Commission. *J. Occup. Med. Toxicol.* **6:2**. (<https://doi.org/10.1186/1745-6673-6-2>)
27. Abernathy B, Hanrahan SJ, Kippers V, Mackinnon LT, Pandy MG. 2005 *The biophysical foundations of human movement*, 2nd ed. South Yarra, Victoria: Palgrave Macmillan.
28. Gasda PJ, Haldeman EB, Wiens RC, Rapin W, Bristow TF, Bridges JC, Schwenzer SP, Clark B, Herkenhoff K, Frydenvang J, et al. 2017 In situ detection of boron by ChemCam on Mars. *Geophys. Res. Lett.* **44**, 8739-8748. (doi:10.1002/2017GL074480)
29. Smedler E, Uhlén P. 2014 Frequency decoding of calcium oscillations. *Biochem. Biophys. Acta.* **1840**, 964-969, 2014. (<https://doi.org/10.1016/j.bbagen.2013.11.015>)
30. Van der Jeugd A, Parra-Damas A, Baeta-Corral R, Soto-Faguas CM, Ahmed T, LaFerla FM, Giménez-Llort L, D'Hooge R, Saura CA. 2018 Reversal of memory and neuropsychiatric symptoms and reduced tau pathology by selenium in 3xTg-AD mice. *Sci. Rep.* **8**:6431. (<https://doi.org/10.1038/s41598-018-24741-0>)
31. Flippo TS, Holder Jr WD. 1993 Neurological degeneration associated with nitrous oxide anesthesia in patients with vitamin B12 deficiency. *Arch. Surg.* **128**, 1391-1395. (doi:10.1001/archsurg.1993.01420240099018)
32. Wu F, Xu K, Liu L, Zhang K, Xia L, Zhang M, Teng C, Tong H, He Y, Xue Y, et al. 2019 Vitamin B12 enhances nerve repair and improves functional recovery after traumatic brain injury. *Front. Pharmacol.* (<https://doi.org/10.3389/fphar.2019.00406>)
33. Young W. 2009 Review of lithium effects on brain and blood. *Cell Transplant.* **18**, 951-975. (<https://doi.org/10.3727/096368909X471251>)
34. Simeoni RJ. 2003 Bohr's model of atomic hydrogen extended to include electron rotational kinetic energy. *Physics in Canada.* **59**, 309-311.
35. Anke M, Croppel B, Kronemann H, Grün M. 1984 Nickel – an essential element. *IARC Sci. Publ.* **53**, 339-365.

ACKNOWLEDGMENTS AND DATA AVAILABILITY

For those interested, the Author welcomes emailed requests for further details relating to the presented Case Study. Similarly, the extended May 9, 2022 "World ME Day version" of this article, that supports the day's theme of #LearnFromME, is also available from the Author.

APPENDIX A – HEAVY METAL OBSERVATIONS

The described quantum treatment approach having some effect on heavy metal levels is not to be expected, especially for relatively short treatment periods. Nonetheless, the human body has some ability for the self removal of heavy metals and interesting observations are revealed when a quantum analysis similar to that of Subsection 8.1 is applied to the 15 heavy metal elements assessed within the Oligo scan. Before presenting analysis results in terms of ranked level changes, it is declared that trends are not as convincing as in Subsection 8.1 (e.g., in terms of the progressive nature of changes) but conversely it is recognised that if any effect is real, then practical limits must apply since continual change without limit would be unreasonable to expect, and unhealthy in the case of increasing levels (which must eventually plateau).

When ranking the heavy metal elements¹⁰ in descending order from largest percentage increase down, the first ranked element for both Scans 3 and 4 is Ni. While the increase is modest (12% and 8% for Scans 3 and 4 respectively), the ranking is somewhat interesting since the reversed mapped value of $\Delta\phi_{Ni} = 140^\circ$ is angularly equivalent to 50° about a landmark Cartesian angle (i.e., $140^\circ = 90^\circ + 50^\circ$) and $\Delta\phi_c = 50^\circ$ equates to one of the eight primary Family members in [18]. Also, the corresponding value of $\bar{\alpha}_{Ni}$ is approximately 30° ($29.44 \pm 0.12^\circ$) which is interesting given the $\Delta\phi = m \times 30^\circ$ multiplicity in table 4. The result may lead one to ponder whether removal of the modern ether, and hence removal of some associated phase interference around 30° , combined with neural stimulation, catalysed some change involving increased Ni uptake or utilisation.

This highest ranking for Ni is also interesting from an essential trace element perspective. That is, Ni deficiency reportedly [35] may disturb skeletal incorporation of Ca, lead to adverse skin effects, and disturb Zn and carbohydrate metabolism. Table 4 seems to indicate disturbed Zn metabolism and skin symptoms are a non-specified (by the present article) aspect of the Case Study. While the initial Ni levels in Scans 1 and 2 are not reported as being excessively low (one of six heavy metals in the normal or green range), one might ask ... *is the modest Ni increase reflecting the commencement of system healing?*

Cd and Pb are the heavy metals with the two highest relative levels (consistently the case for Oligo Scans 1 to 4, both being in the high plus yellow but not excessive range). Furthermore, the highest-to-lowest ranking topped by Ni places Pb last for both Scans 3 and 4 (i.e., on average Pb levels reduce by the most). Even more interesting than the Ni 50° angular outcome is the fact that $\Delta\phi_{Pb} = 410^\circ$ is solely equivalent to 50° (i.e., $360^\circ + 50^\circ$). The above observations are summarised by table A1, which as per Subsection 8.1

¹⁰Al is omitted from the analysis due to the previously noted adversely appreciable increase in its level (which had reduced from Scans 3 to 4).

possibly provides a glimpse from a quantum mechanical perspective as to why heavy metals interfere with processes involving essential elements (the table also includes related Ag and Gd observations).

Table A1. Heavy metal elements with the most notable level change when comparing post-treatment Oligo Scan 4 with the average values of pre-treatment Scans 1 and 2. Also selectively given are $\Delta\phi$ values (deconstructed), and a notable corresponding $\bar{\alpha}_{\Delta\phi}$ value for Ni as predicted by reverse mapping.

Basis for element inclusion	Element	Z	$\Delta\phi$ (degrees)	Model $\bar{\alpha}_{\Delta\phi}$ (degrees)
Largest % increase	Ni	28	140 (90+50)	29.44 ± 0.12
Largest % decrease	Pb (1 st)	82	410 (360+50)	
	Ag (2 nd)	47		
	Gd (3 rd)	64	320 (270+50)	

Supportive of the high Cd levels across Scans 1 to 4 is a hair toxicology test of March 2021 (with analysis performed within the Environmental Analysis Laboratory, Southern Cross University, by a commercial provider – result ID: K3573-1). The analysis highlights Cd as being the only heavy metal in the provider’s defined red zone, with a level of 0.062 mg/kg being approximately three times a population average and just falling into said zone. More than one health practitioner, including my CFS specialist physician, has suggested the possibility of heavy metals adversely replacing desirable elements at the cellular level and within the Krebs cycle. Noting that Cd vertically proceeds Zn in Group 12 of the periodic table (and therefore has the same outer-most subshell electron configuration of $d^{10}s^2$), and that Zn and Cd both have Z values that are integer multiples of 3 (recall that Subsection 8.1 quantum findings arose from the observation that all Z values in table 4 are integer multiples of 3), some Cd-based disturbance as a contributing CFS factor for the presented Case Study may be indicated.

The identification of Ag in table A1 is interesting given the controversy surrounding colloidal Ag supplements, but again it is not appropriate or possible to draw conclusion from the tentative result.

APPENDIX B – SUPPLEMENTARY REVERSE MAPPING RESULTS

This Appendix contains further outcomes from the reverse mapping modus operandi of Subsection 6.2 (i.e., applies the $\Delta\phi_c/5 \rightarrow z \rightarrow Z$ transformation in reverse). Here, the reverse mapping is applied to all elements from Z = 1 to 63,

and then only selects those with a median $\bar{\alpha}_{\Delta\phi}$ value, as generated by (1), that falls within 0.5% of some integer, or integer multiple of a fraction ($\frac{1}{3}$ or $\frac{1}{4}$), when expressed in units of degrees.

Interestingly, table B1 contains several of the "usual suspect" elements from the main discussion. Note that as explained in Subsection 8.1, predicted $\bar{\alpha}_{\Delta\phi}$ values given in table B1 are taken as falling exactly on the $\bar{\alpha}_{\Delta\phi}$ versus $\Delta\phi_c$ model curve of figure 3, whereas in [18] all Family $\bar{\alpha}_{\Delta\phi}$ values fall slightly off the model curve. Hence, the predicted $\bar{\alpha}_{\Delta\phi}$ value for Ar in table B1 differs slightly from the corresponding value stated in [18]. Several intriguing aspects of table B1 exist but are not pursued here (e.g., the noble gas elements of Ar and Xe having landmark $\Delta\phi$ values of 90° and 270° respectively, and linkage of some of the heavier elements via a known decay chain).

The primary reason for identifying elements with integer-related $\bar{\alpha}_{\Delta\phi}$ values within table B1 is that there is an uncanny integer connectedness for $\bar{\alpha}_{\Delta\phi}$ values in the main table 4. It may well be that this connectedness is an all-for-one chance occurrence. Viz., if the ratios of $\bar{\alpha}_{\Delta\phi}$ values display fractional connectedness, as in [18], then one by-chance absolute alignment (to within 0.5% as specified) would result in alignment for all (the previously explained $\alpha_{\min} \approx 0.1740^\circ$ that applies across all Families in [18] is also suggestive of some universal linkage). The non-SI unit of degree is an artificial construct and so no obvious reason exists as for why $\bar{\alpha}_{\Delta\phi}$ values would align with such a construct. Regardless, alignment exists and amidst the complexity of the modern ether there may well be indirect fractional-integer phase modulations comparable to the $\bar{\alpha}_{\Delta\phi}$ values of table B1 (since RF communication transmissions routinely contain ordered arrays of integer spaced quantities, and digital phase-shift keying schemes certainly employ integer amounts of degrees in their discrete phase shifting). Hence, the two right-most columns of table B1 are worthy of reporting.

Table B1. $\Delta\phi_c$ and corresponding $\bar{\alpha}_{\Delta\phi}$ values predicted by reverse mapping of elements from Z = 1 to 63 and for which generated (median) $\bar{\alpha}_{\Delta\phi}$ values fall within 0.5% of some integer, or integer multiple of a fraction ($\frac{1}{3}$ or $\frac{1}{4}$), when expressed in units of degrees. Uncertainties are stated at 95% CI.

Z	Element	$\Delta\phi$ (degrees)	Model $\bar{\alpha}_{\Delta\phi}$ (degrees)	± (degrees)	Nominal $\bar{\alpha}_{\Delta\phi}$ (degrees)	Deviation (%)
9	F	45	0.2510	0.0075	¼	0.40
15	P	75	0.6631	0.0121	⅓	-0.53
18	Ar	90	1.0026	0.0148	1	0.26
29	Cu	145	3.0087	0.0265	3	0.29
30	Zn	150	3.2504	0.0277	¾	0.012
31	Ga	155	3.5020	0.0289	¾	0.057
46	Pd	230	8.4619	0.4484	8½	-0.45
53	I	265	11.5377	0.3281	11½	0.33
54	Xe	270	12.0167	0.1391	12	0.14
55	Cs	275	12.5055	0.0442	12½	0.044
56	Ba	280	13.0042	0.0327	13	0.033
57	La	285	13.5129	0.0952	13½	0.095
58	Ce	290	14.0314	0.2239	14	0.22